ELSEVIER

Thin Solid Films 389 (2001) 116–137

thin solid films

www.elsevier.com/locate/tsf

Structural variants in heteroepitaxial growth

C.P. Flynn[a,*], J.A. Eades[b]

[a] *Physics Department, Materials Research Laboratory, University of Illinois at Urbana-Champaign, 1110 W. Green Street, Urbana, IL 61801, USA*

[b] *Department of Materials Science and Engineering, Lehigh University, Bethlehem, Pennsylvania 18015-3195, USA*

Received 15 May 2000; received in revised form 8 December 2000; accepted 14 December 2000

Abstract

The occurrence of structural variants during epitaxial growth is examined using two-dimensional symmetry. The modeling of the materials includes equilibrium defect structures and reconstructions in addition to epitaxial strain and flaws. Specific results are presented for single and multi-terrace systems and for miscut substrates. Analytical results for planes on which variants nucleate in equal proportions are obtained simply, from two-dimensional symmetry arguments. These are used to discuss ways to inhibit the growth of unwanted variants. © 2001 Elsevier Science B.V. All rights reserved.

Keywords: Symmetry; Epitaxial variants; Surface structure

1. Introduction

This paper concerns structural variants that form, in proportions defined in part by symmetry, during the epitaxial growth of materials on single-crystal substrates. Epitaxial growth presents unique opportunities for the synthesis of materials with scientific importance and technical value. Accordingly, we seek an improved understanding of the fundamental limits that constrain epilayer structure. Here, and in what follows, the term structural variant refers to distinct regions of an epilayer with different configurations that are related to each other by a crystal symmetry operation of the substrate such as rotation or reflection. A particular example is GaAs grown on a Ge (110) substrate, where two structural variants of GaAs grow on Ge (110) with equal abundance, and differ only by occupying the two sublattices with Ga and As interchanged. A second example occurs when a f.c.c. (111) epilayer grows on the (0001) surface of a substrate with hexagonal symmetry, so that two f.c.c. structural variants, respectively, stacked ABCA... and ACBA... are created by symmetry with equal probabilities. In the first example the structural variants are related by inversion (among various alternative descriptions) and in the second by reflection as twins; other possible variant relationships are discussed below. Here we develop a convenient framework to describe the proportions of structural variants for a given epilayer on any substrate crystal.

While variants offer behavior of theoretical interest their practical role is largely as a nuisance to be avoided where possible. Variants alter physical properties, creating recombination centers in semiconductors, for example, and residual resistance in metals, while generally reducing crystalline coherence. Copper grown by heteroepitaxy generally is broken into stacking domains ~ 1 μm in extent, whereas in a bulk crystal the presence of a single twin which creates regions with alternative stackings is a matter for note. This occurs in an epilayer when the substrate lacks the template required to select among variants, so that several variants nucleate and grow. Then interest turns to properties such as substrate miscut that break the symmetry and suppress

* Corresponding author. Tel.: +1-217-2446297; fax: 1-217-2442278.
E-mail address: cpt@uimrl17.mrl.uiuc.edu (C.P. Flynn).

PII: S0040-6090(01)00768-4

unwanted variants. This paper employs symmetry to find rules that guide future experiments in the choice of substrates that select particular variants.

A general theory of interfaces has been developed and applied to variants in epitaxial systems. This has grown out of research starting with Van Tenderloo and Amelinckx [1], and subsequently several other groups [2–17], but primarily Pond and colleagues [2–13], in research reviewed by Sutton and Balluffi [18]. The Pond theory uses the symmetry of the Shubnikov groups that describe the dichromatic complex of two interpenetrating bulk lattices to predict the occurrence of variants. As explained by Sutton and Baluffi [18], this approach finds precise applications to grain boundaries and interfacial line defects in general [19,20]. It is presented by Sutton and Baluffi [18] as describing epitaxial variants in all particular cases. Thus, the variant populations are thought to follow from the symmetry classifications of the bulk crystals, together with the interface orientation. Limitations on the degree to which this is true provides one of the topics addressed in the present paper. A success of the theory is an analytical result, in the case of GaAs on Ge discussed above, that two GaAs variants occur equally not only on Ge (110) but also on all Ge {hk0} surfaces for arbitrary h and k.

Our contrary view is that heteroepitaxy requires the growth of epilayer material on a specific surface and that the structure of that surface then determines epilayer properties such as variant distributions. The relevant surface characteristics include first its symmetry, and others (such as miscut and multiterrace structure) that remain in some degree amenable to symmetry arguements, but also those (such as misfit) which cause complication that remain to be accommodated. As a particular example, GaAs does *not* grow with two equivalent variants on Ge {hk0} (the Pond result). Instead, the two variants grow with a spatially heterogeneous distribution that depends on the multi-level character of the substrate, the vicinal miscut, and the size of the variants relative to the substrate terrace width. Specific questions of epitaxial structure thus, intrude into the consequences of symmetry.

Here we begin from the observation that the surface cuts irrevocably break the bulk symmetries of the substrate and epilayer crystals. Only the symmetry of the resulting truncated crystals is relevant to heteroepitaxy and the occurrence of variants. By treating only the remaining symmetry we gain the twin advantages of greatly restricting the scope of the discussion from three-dimensional to two-dimensional space groups, and at the same time making direct contact with the surface terrace structures that most influence heteroepitaxy. The resulting simplification allows the variants for all possible substrates and epilayers, given an interface formed from planar terraces, to be enumerated in Section 2 as a single table spanned by the symmetries of the substrate and epilayer surfaces. In Section 3 this same approach allows us to treat the heterogeneity in variant distribution caused by multilevel behavior, and to optimize variant selection, when the crystal has a basis of more than one atom per lattice point. The important effects of vicinal miscut as a means to control and suppress variant populations are treated in Section 4. A further advantage of reduced dimensionality in the variant problem is the global perspective that emerges on the general extent to which practical systems are affected by symmetry factors. We emphasize that the results presented here could equally be deduced from the relevant three-dimensional symmetries, after the two interface orientations are, in addition, specified (in effect, the three-dimensional symmetries and the surface cuts fix the surface symmetries). However, the 230 distinct space groups in three-dimensions, and the multiplicity of cuts for each of the substrate and epilayer, had evidently created a barrier to any exploration of useful catalogs of behavior.

It requires mention that the full epilayer crystal structure remains necessary to specify the details of boundaries among variants, and other defects [19,20].

In connection with a comparison of two-dimensional and three-dimensional descriptions we mention also that the actual symmetry of an epilayer generally differs from that of the bulk. While the substrate is normally of macroscopic dimensions, and usually unstrained, the epilayer is a thin film with strains determined by interactions with the much stiffer substrate. It is a fact, for this thin film geometry, that interfacial tractions from size misfit or differential contraction with the substrate lead to strain fields that are *uniform* through the thickness of the epilayer. A simple example is a cubic epilayer material grown (001) on a square substrate surface lattice, which will normally grow tetragonal with the *c*-axis perpendicular to the interface. Thus, the three-dimensional symmetry of the actual epilayer is different from that of the bulk material. Therefore, it is essential to determine an epilayer symmetry only *after* the surface cut and eventual strain fields are fixed. Specifically, the relevant 'bulk' epilayer symmetry is in part determined by the surface cut itself, and is not available until the interface orientations are fixed. A particular example is h.c.p. Dy grown (0001) on h.c.p. Lu (0001) [21], for which the isotropic epitaxial misfit causes the Dy to magnetize and actually become orthorhombic, with three structural variants that correspond to the three in-plane magnetization axes (there are six magnetic variants, two magnetic directions for each structural axis). The magnetized phase does not occur when Dy is grown on h.c.p. Y (0001) [22], as it originates entirely from epitaxial strain. In the present treatment the Lu (0001) substrate is assigned a 3-m

surface symmetry, and the orthorhombic epilayer a 2-mm surface symmetry, from which the existence of three variants follows directly. Quick, intuitive and accurate recognition of variant properties is of particular value in an experimental setting. This two-dimensional approach to variant enumeration forms the core of Section 2.

Given the surface symmetries, an elegant and readily accessible basis for treating epitaxial variants is available, following the original discussion by Van Tenderloo and Amelynckx [1] of the separate but similar problem of variants that appear as localized precipitates in bulk crystals. Here the same ideas are adapted to the two-dimensional symmetries of epitaxial systems, which requires only the simplest methods. Simplicity is especially desirable for epitaxy because scores of practical cases arise in which, using the language of two-dimensional symmetry employed here, the symmetry analysis may be completed by inspection alone, and for others only a small further framework of theory is needed.

It is important to recognize that epitaxy is complicated far beyond the point at which *any* exact structural symmetries remain. Heteroepitaxial growth begins with nucleation, often far from equilibrium, and often is complicated by competition among several mechanisms [23–26]. Even in favorable cases it is hard to predict beforehand what will grow from a particular flux of materials supplied to a substrate material maintained under specified conditions [27]. Variants may be seeded from the initial epilayer deposition on the substrate crystal. During early phases, precursors of variants grow at distinct positions, both by accretion and by kinetic competition, and the final configuration may evolve during post-growth processing without further deposition. Nucleation may occur at step edges, at extrinsic or intrinsic (activated) flaws, or on the template terraces. A number of chemically inequivalent epitaxial overgrowths may form simultaneously. Growth may take place where a substrate is deformed, defective or reconstructed, so that the local structure differs from that of the truncated bulk crystal. Often, the initial monolayer is pseudomorphic and the final structure forms by reconstruction after several layers of growth. A metastable structure may persist for hundreds of monolayers [28]. Kinetic factors limit the degree to which an epilayer achieves equilibrium; glassy films are an extreme case [29]. The epilayer structure may change during annealing or cooling, or through differential contraction or applied fields. The symmetry of real materials is broken by surface reconstructions and mobile surface defects. Only very thin epilayers retain any possibility of remaining exactly commensurate with the substrate surface periodicities; all others are incommensurate, and this affects the behavior of translational variants.

In the face of this complexity, a study of symmetry constraints might at first appear unpromising. To the contrary, symmetry survives the complexity, and certain accurate statements may still be made about the way symmetry constrains the growth of variants.

It captures the essence of epitaxy to organize the subject matter with emphasis on low index planes and the behavior of extended terraces. Almost all epitaxial research employs low index planes of the substrate material. These possess a high areal density of atomic cells that tends to nucleate low index planes of the epilayer, and are separated by correspondingly high step edges. Accordingly, the symmetry of variants warrants interest largely for low index surfaces as, indeed, is true of epitaxy more generally. The results often differ for single terrace, multi-level and vicinal surfaces, and these are the topics of Sections 2–4, respectively. In Section 2, the variant populations are enumerated for all possible symmetries of the substrate and epilayer terraces. Section 3 treats multilevel behavior with particular regard to the opportunities it presents for suppressing subsets of variants. Section 4 is focused on the way miscut can be employed to enhance the population of any selected variant. The treatment in Sections 2–4 concerns idealized models that neglect the complications of real systems, detailed above. Section 5 then considers the degree to which the results are sensitive to such physical factors as thermally activated surface structure, lattice strain, and incommensurability between the substrate and epilayer structures. Section 6 suggests how the results of the paper may be employed in practice.

2. Symmetry and the variants on a single terrace

This section treats the way symmetry determines what variants form on a given terrace. Section 2.1 defines the lattices of the substrate and epilayer crystals. Section 2.2 defines substrate symmetry for idealized materials, and Section 2.3 treats epilayer symmetry. Variant enumeration and global symmetry are the topics of Section 2.4 and Section 2.5 summarizes the results. The accommodation of thermal defects and structural flaws within this framework is the topic of Section 5.

2.1. Substrate and epilayer crystals

The simplest substrate consists of a crystal that is terminated by an indefinitely extended terrace unbroken by step edges. Possible thermal or athermal flaws in this terrace are treated in Section 5. The unperturbed Bravais crystal lattice of the substrate is spanned by basis vectors $\mathbf{a}_1^s$, $\mathbf{a}_2^s$, $\mathbf{a}_3^s$, that define [30] the reciprocal lattice vectors $\mathbf{b}_1^s$, $\mathbf{b}_2^s$, $\mathbf{b}_3^s$, by $\mathbf{b}_1^s = 2\pi\ \mathbf{a}_2^s \times \mathbf{a}_3^s/\Omega$, etc., with Ω the volume of the unit cell. The

substrate terrace treated here is defined by the reciprocal lattice vector

$$\mathbf{g}_s(h,k,l) = h\mathbf{b}_1^s + k\mathbf{b}_2^s + l\mathbf{b}_3^s \quad (1)$$

with h, k, l, integers with common factors removed. The distance between (h,k,l) planes is

$$d(h,k,l) = 2\pi/|\mathbf{g}_s| \quad (2)$$

In more complex crystals the several atoms per unit cell require, in addition, position vectors $\boldsymbol{\rho}_s$ to locate them relative to the Bravais lattice point.

The Bravais *surface* net of the substrate is defined by new basis vectors $\boldsymbol{a}_2^s$, $\boldsymbol{a}_3^s$, that contain integral multiples of the lattice basis vectors, together with an interplanar vector $\boldsymbol{a}_1^s$. The corresponding reciprocal lattice vectors are $\boldsymbol{b}_1^s$, $\boldsymbol{b}_2^s$, $\boldsymbol{b}_3^s$. Here, italic letters are employed for the vectors related to a particular choice of surface plane $\mathbf{g}_s(h,k,l) = \boldsymbol{b}_1^s$. The surface net $\boldsymbol{a}_2^s$, $\boldsymbol{a}_3^s$, is not defined uniquely owing to the multiplicity of ways it can be specified. $\boldsymbol{a}_2^s$, $\boldsymbol{a}_3^s$ may be selected for shortness and angular separation, and similar criteria employed in the choice of $\boldsymbol{a}_1^s$.

An epilayer is similarly specified by bulk basis vectors $\mathbf{a}_1^e$, $\mathbf{a}_2^e$, $\mathbf{a}_3^e$. Ordinarily its surface normal along $\mathbf{g}_e$ is parallel to $\mathbf{g}_s$(h, k, l) but the two have differing lengths that correspond to the different plane spacings in the epilayer and substrate. The basis vectors of the *surface* net, $\boldsymbol{a}_2^e$, $\boldsymbol{a}_3^e$, contain multiples of the bulk basis vectors $\mathbf{a}_1^e$, $\mathbf{a}_2^e$, $\mathbf{a}_3^e$, as also does the third vector of the set, $\boldsymbol{a}_1^e$. Epitaxy is usually determined by the fit between $\boldsymbol{a}_2^e$, $\boldsymbol{a}_3^e$, and one or both of $\boldsymbol{a}_2^s$, $\boldsymbol{a}_3^s$.

The variants on which this paper is focussed all have basis vectors equivalent to $\boldsymbol{a}_1^e$, $\boldsymbol{a}_2^e$, $\boldsymbol{a}_3^e$, such that the structure is merely rotated, mirrored or translated from one variant to the next. They all have equivalent chemical relationships to the substrate. These matters are quantified below. Variants are mutually distinguishable, as their atomic positionings differ, and detectable interruptions of crystal structure occur at boundaries where two variants meet (see Sutton and Balluffi [18]), as illustrated in Fig. 1. Two matters require mention here. First, the epilayer surface net $\boldsymbol{a}_2^e$, $\boldsymbol{a}_3^e$, normally differs not only from the substrate net but also from that of the *un*strained bulk epilayer material. The variants are thus strained, which may *change their symmetry*. Thick films also are incommensurate with the substrate, which can make translational variants unrecognizable. This point is discussed further in Section 5 after the symmetry results are established. Second, typical substrates do not have flat surfaces but instead comprise terraces, spanned by $\boldsymbol{a}_2^s$, $\boldsymbol{a}_3^s$, and connected by out-of-plane vectors. Fig. 1a,b shows the two limits in which the typical variant size D is respectively much less than and much greater than the terrace length L. In effect the former case with $D \ll L$ provides the subject matter of this section, as each variant is determined by a single terrace. The translation vectors $\boldsymbol{a}_1^s$, $\boldsymbol{a}_1^e$, between terraces generally differ for the substrate and the epilayer, which relates to the matter of translational variants mentioned above (Section 5). Translations among terraces may contain position vectors, $\boldsymbol{\rho}_s$, in addition to basis vectors like $\boldsymbol{a}_1^e$, with consequences for interfacial chemistry that are discussed in Sections 3 and 5.

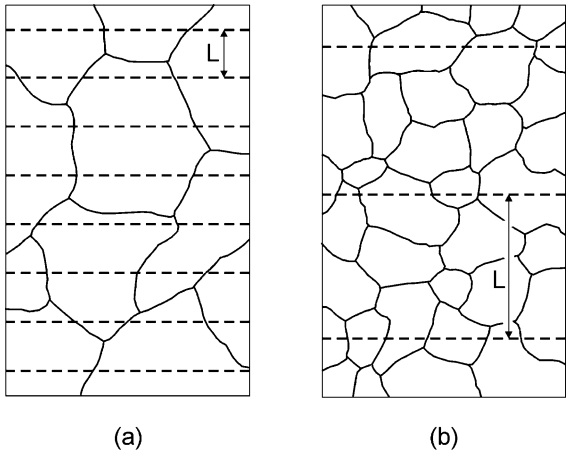

Fig. 1. Variant structures. In (a) the variants are large and overlap onto several terraces, as indicated by the broken lines spaced by L that mark step edges. In (b) the variants are smaller than the terraces. For clarity, the steps shown are unrealistically regular.

2.2. Symmetry of an ideal single-terrace substrate

Suppose that the substrate is cut from an infinite, perfect crystal that has translational invariance from cell to cell, as defined by the basis vectors $\boldsymbol{a}_1^s$, $\boldsymbol{a}_2^s$, $\boldsymbol{a}_3^s$ introduced above, and also possesses symmetry about sites in the unit cell. The symmetry is a catalog that includes rotations, reflections, inversions in addition to operations such as glide planes and screw axes that relate to the structure of the basis [31,32]. The substrate we consider is semi-infinite, with the free surface cut exactly along a crystal plane, and all atoms at exact lattice positions. Therefore, translational invariance in the plane is retained, with basis vectors $\boldsymbol{a}_2^s$, $\boldsymbol{a}_3^s$. Whether or not any point symmetry remains about surface sites depends on the particular crystal and the plane (h,k,l).

The 10 alternative point symmetries available to the substrate are the two-dimensional crystallographic point groups [32]. They contain all symmetries of the infinite crystal that are not destroyed by the surface cut. The symmetry operations include only those rotations with axes parallel to the surface normal, and mirror planes with normals that lie in the plane of the surface. Specifically, the first five comprise the rotations of order 1, 2, 3, 4 and 6, indicated conventionally by the

relevant integer, and the remainder are the same rotations but with a mirror, written m, 2mm, 3m, 4mm and 6mm. Rotations and mirrors act together. For example, a twofold rotation with a mirror creates *two* mirror planes, hence the notation 2mm. Successive terraces of a crystal possess the same symmetry, but a multi-atom basis can cause successive terraces to differ in structure.

Crystals with a multi-atom basis may have screw axes or glide planes. If the surface plane cuts the translation vector of the screw or glide the symmetry operation is broken. Screws and glides are, therefore, ignored, except a glide plane with its translation parallel to the surface. The modified treatment for multilevel surfaces is explained in Section 3.

In addition to these overt symmetries, the substrate material retains latent symmetries that constrain its more general behavior, as described in Section 5.

2.3. Symmetry of an ideal epilayer

The symmetry description of an epilayer required for an enumeration of epitaxial variants is analogous to that given above for the substrate symmetry, specifically the 10 two-dimensional point groups, the translational symmetry, and any glide plane in the surface plane. Owing to a subtlety concerning translational variants, explained in Appendix A, an epilayer screw axis oriented normal to the interface is to be treated for variant enumeration on a single terrace as a simple rotation axis, and a glide plane perpendicular to the surface is treated as a simple mirror. There are additional factors which are now explained with the help of illustrative examples.

2.3.1. Three-dimensional structure

A slab-like epilayer can display certain additional symmetry elements related to its three-dimensional structure that are not contained in the present two-dimensional description, but these play no part in variant enumeration and are detailed in Appendix A. The epilayer and substrate symmetries treated here nevertheless are two-dimensional symmetries *of the three-dimensional material*, not of the surface planes alone, because interatomic forces can modify chemical equivalence through multiple atomic planes. An f.c.c. (111) surface is threefold with a mirror (3m) even though the surface layer of the truncated bulk has close packed sites with (6mm) symmetry. The observed occurrence of variants can monitor the degree to which deeper layers do, in fact, influence variant energies. For example, strong effects occur for Si (001), for which the bulk-terminated surface is square, but this symmetry is broken by bonding from below which leaves the actual surface twofold with a mirror (2mm), and which in turn causes 'dimer row' reconstructions [33] along [110] and [1$\bar{1}$0] on successive terraces.

2.3.2. Strain

When an epilayer forms on the substrate, both materials may be modified by the interaction, but most commonly the epilayer, and in particular its symmetry may be changed. This happens because the in-plane spacing of epilayer atoms depends on the interaction with the substrate during growth. The resulting strains extend through the epilayer as discussed in Section 5. The epitaxial strain can influence the epilayer symmetry directly, as in the breaking of cubic symmetry, and also indirectly by creating a different phase which has its own symmetry; conversely the epilayer can change the substrate. These processes warrant clarification by specific examples. In Section 1 the case of phase change is illustrated by helimagnetic h.c.p. Dy (0001) grown on h.c.p. Lu (0001) [21], where the Dy magnetizes to become orthorhombic and creates three structural (six magnetic) variants. The strain-induced transitions thus, break the symmetry both of the unstrained epilayer and of the epitaxial strain. As the example of Dy on Lu makes clear, the epilayer symmetry relevant to variant enumeration is that of the material as it exists in the actual variant. A final complication is that epitaxial strain may take the epilayer into a two-phase region of the phase diagram, where alternative structures necessarily coexist in thermal equilibrium, but as this necessarily deals with more than one epilayer crystal structure it lies outside the scope of the present discussion.

2.3.3. Reconstructions

A further example of modified epitaxial symmetry occurs when either or both of the substrate and epilayer surfaces reconstruct. Also, interfacial reconstructions may be induced by their mutual interaction. Of many examples in which epilayers modify the substrate surface we mention that alkali [34] and oxygen [35] monolayers induce 'missing row' reconstructions on (011) surfaces of f.c.c. metals such as Cu, Ni, Pt, with complementary structure of the overlayers. Reconstructions are treated in Section 5.1. The conclusion there is that substrate reconstructions are to be ignored because, on average, they occur equally in all symmetry-related orientations of the substrate contained in the normal enumeration of variants (see Section 2.4). When an epilayer is deformed by a reconstruction of the interface with the substrate it would certainly be consistent to employ the epilayer symmetry as deformed (since there are distinct interfacial structures), and to recognize interfacial variants. We prefer instead to distinguish between (1) variants as distinct bulk structures and (2) reconstructions as distinct structures confined to the interface. With this definition all

reconstructions are ignored in the assignment of substrate and epilayer symmetry.

2.3.4. Summary of symmetries

Variants are required to be chemically equivalent in their internal structures and their interactions with the substrate. The definition of epilayer symmetry pertains to the uniformly strained state, specifically of the three-dimensional structure near the interface in the case of inhomogeneous material, but excludes deformations confined to the interface.

2.4. Enumeration of variants for a single terrace

Here we treat successively the rotation, mirror and translational symmetries permitted to substrates and epilayers.

2.4.1. Rotation axes

The five rotational symmetries identified above are labeled by the number of equivalent orientations as 1, 2, 3, 4 and 6. Under the action of these rotations, a line drawn on a surface with a n-fold rotation axis generates n equivalent lines at angles of $2\pi p/n$, with p integral. Similarly, when the epilayer in one of its orientations replaces the line there are generated n equivalent epilayer configurations on a surface with an n-fold rotational axis. These need not all give distinguishable crystal structures. If the substrate has a threefold axis (Fig. 2) the epilayer occurs in three orientations; but if the epilayer also has a threefold axis the three arrangements are identical and there is only one variant. In short, the rule is that each new variant is the result of a symmetry operation (or combination of operations) present in the substrate that is not present in the epilayer symmetry [1].

2.4.2. Mirrors

The remaining five point symmetries available to substrates are obtained by combining each of the rotations discussed above with a mirror that contains the rotation axis. The mirror increases the number of symmetry-equivalent configurations by a factor of two, and so the number of variants is increased by a factor of two. The variants then occur in pairs related by reflection in the substrate mirrors. If the epilayer possesses the same mirror, however, the new atomic arrangements of the epilayer that are introduced by the substrate mirror no longer remain distinguishable. The factor 2 is lost and the number of variants is unchanged by the mirrors. The rule once more is that only operations introduced by the substrate that are absent from the epilayer can create new variants.

Table 1 summarizes the number of variants for all possible symmetries of the substrate and epilayer terraces. The maximum number of variants is 12 and the least is, of course, 1. It is an attribute of the two-dimensional description of variants employed here that the results for all cases can be presented so compactly.

Note, as in Fig. 3, that an epilayer mirror can cancel a substrate mirror only if the two mirrors are perfectly parallel. Two examples are cited here to make this requirement concrete. First, in the growth of close packed monolayers of rare gases [36,37] on certain close packed substrates, it is found that the close packed directions in the substrate and epilayer planes differ by a rotation angle of several degrees. As the substrate and epilayer mirrors are thus misaligned there

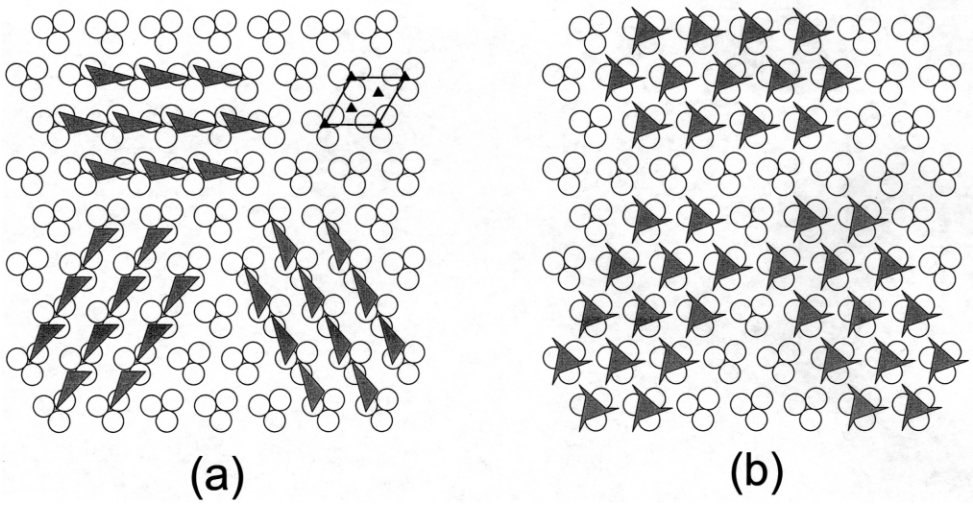

Fig. 2. (a) An epilayer that lacks symmetry (e.g. grey triangles), on a substrate with a threefold axis, occurs in three distinguishable variants; but when in (b) the epilayer also possesses a threefold axis there is only one distinguishable configuration (bottom). The unit cell and its threefold axes are shown in (a).

Table 1
The number of variants formed in epitaxial growth, listed by symmetry of the substrate, S, and epilayer, E, and with the global symmetry given in parentheses[a]

E	S	1	m	2	2 mm	3	3 m	4	4 mm	6	6 mm
1		1 (1)	2 (m)	2 (2)	4 (2mm)	3 (3)	6 (3m)	4 (4)	8 (4mm)	6 (6)	12 (6mm)
m		1 (m)	1 (m)	2 (2mm)	2 (2mm)	3 (3m)	3 (3m)	4 (4mm)	4 (4mm)	6 (6mm)	6 (6mm)
2		1 (2)	2 (2mm)	1 (2)	2 (2mm)	3 (6)	6 (6mm)	2 (4)	4 (4mm)	3 (6)	6 (6mm)
2 mm		1 (2mm)	1 (2mm)	1 (2mm)	1 (2mm)	3 (6mm)	3 (6mm)	2 (4mm)	2 (4mm)	3 (6mm)	3 (6mm)
3		1 (3)	2 (3m)	2 (6)	4 (6mm)	1 (3)	2 (3m)	4 (12)	8 (12mm)	2 (6)	4 (6mm)
3 m		1 (3m)	1 (3m)	2 (6mm)	2 (6mm)	1 (3m)	1 (3m)	4 (12mm)	4 (12mm)	2 (6mm)	2 (6mm)
4		1 (4)	2 (4mm)	1 (4)	2 (4mm)	3 (12)	6 (12mm)	1 (4)	2 (4mm)	3 (12)	6 (12mm)
4 mm		1 (4mm)	1 (4mm)	1 (4mm)	1 (4mm)	3 (12mm)	3 (12mm)	1 (4mm)	1 (4mm)	3 (12mm)	3 (12mm)
6		1 (6)	2 (6mm)	1 (6)	2 (6mm)	1 (6)	2 (6mm)	2 (12)	4 (12mm)	1 (6)	2 (6mm)
6 mm		1 (6mm)	1 (6mm)	1 (6mm)	1 (6mm)	1 (6mm)	1 (6mm)	2 (12mm)	2 (12mm)	1 (6mm)	1 (6mm)

[a] The results are valid for substrates that are Bravais lattices, and for single terraces of any other substrates. For multilevel surfaces, the results hold provided that screw axes normal to the surface are treated as simple rotation axes, and glide planes that contain the surface normal are treated as simple mirrors. For the 25 cases in which both the substrate and epilayer symmetries include mirrors it has been assumed that these mirrors are parallel. If they are not parallel the number of variants is doubled, but the global symmetry remains unchanged. Screw axes can alter the global symmetry of an entire epilayer as explained in Section 3.5.

result two variants; these correspond to opposite angular displacements of the Ar. Similarly, rare earth $(1\bar{1}02)$ epilayers grow on Nb (211) with the normal to the epitaxial plane reoriented by a 'tuned tilt' [38] of a few degrees from the Nb (211) normal. Two tilted variants then become detectable, rotated from each other by an in-plane angle π. In the absence of this tilt, the Nb (211) and rare earth $(1\bar{1}02)$ have parallel mirror planes, the two atomic arrangements are identical and a single variant is the result. Thus, exactly parallel mirrors are required to eliminate a possible new variant.

2.4.3. Global symmetry

It is convenient at this point to define a *global symmetry of the variants* that is characteristic of an ensemble of variants grown on a surface. Questions of probe size then enter the discussion of observed symmetry. A probe restricted to one variant generally detects a different symmetry from a probe that samples a statistical distribution of variants. The different variants, being equivalent on each terrace must, on average, form in equal proportions. Therefore, the global symmetry is the superposition of the symmetries of all

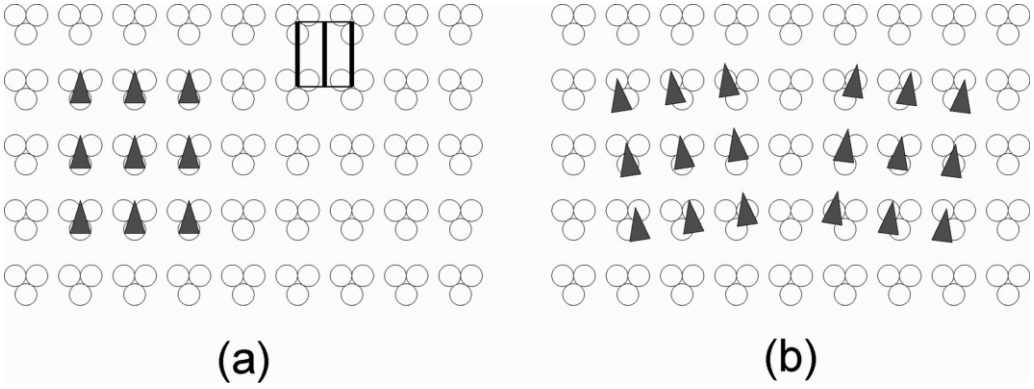

Fig. 3. When the substrate and epilayer each contain a mirror, as in the examples shown, only one variant occurs when the mirrors are exactly parallel, as in (a); otherwise there are two distinguishable variants (b). Mirrors of the unit cell are shown by thick lines in (a).

the variants. Since the variants contain all symmetries of the substrate that are lacking from the epilayer crystal, the global symmetry is, in short, the union of the epilayer and substrate symmetries. This is the expected symmetry for the diffraction pattern of all variants on a terrace. The global symmetries for given epilayer and substrate symmetries are represented in Table 1. In Section 3 it is shown that, in the special case where the atomic basis introduces a screw axis parallel to $\mathbf{g}_s(h,k,l)$, the global symmetry includes also the rotational order of that axis.

2.4.4. Translations

Given a substrate with q equivalent nucleation sites for the epilayer there are q translational variants for each of the point variants identified in Table 1. For example, scanning tunneling microscopy has been employed [39] to examine the growth of oxygen monolayers on W (110), including the eight variants of the (2×2) phase, and the observable boundaries, that occur near 75% coverage. In the growth of the perovskite $BaTiO_3$ (100) on Mg using a first layer of rutile TiO_2 to satisfy interfacial electrostatic requirements [40], the resulting perovskite similarly exists in four translational variants. To the degree that the substrate translational and other symmetries are independent of each other, the total of variants is obtained as the product of the q translationals and the result from point symmetries in Table 1.

Note that the separation into translational and other symmetries of variant is not always trivial. This is illustrated by the case of a hexagonal substrate in which, say, successive layers occupy A-type sites of a hexagonal net, with B and C sites unoccupied. If the epilayer also occupies only A sites there are no translational variants and Table 1 gives the number of variants. If, instead, the epilayer occupies hollow sites, the B and C sites are degenerate, and have threefold symmetry with a mirror. An epilayer whose only symmetry is to share the substrate mirror then has three rotational variants for each type of site. Nevertheless, since the two sites differ by a rotation of π in addition to a displacement, the six variants can still be distinguished by orientation alone and regarded, if so desired, as purely rotational variants, ignoring the coupled translation. For a twofold epilayer with the same mirror, however, the two types of site can no longer be identified by orientation, and there remain two translational variants for each of three orientations. An epilayer which is threefold with a mirror, on the other hand, occurs rotated by π at the two available sites, and the variants are equally translational and rotational in character. These examples are clarified in Fig. 4. For substrates that are h.c.p. or f.c.c., rather than hexagonal, the B and C sites are no longer degenerate owing to the stacking, and translational variants are thereby eliminated. The discussion neglects the further possibility that a higher-order transition to off-center sites creates added translations. We conclude that translations can occur with peculiarities that require examination case by case. This is reinforced in Section 5 by consideration of the extent to which translations remain detectable in the face of strain and incommensurability.

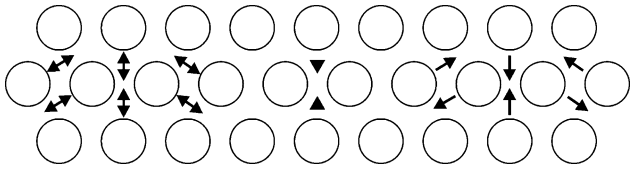

Fig. 4. Translational variants occupying threefold sites of a hexagonal substrate. The variants are indicated by symmetry symbols in the sites they occupy. On the left are six variants whose only point symmetry is a mirror parallel to the substrate mirror; on the right are the six variants with a twofold axis and the same mirror; in the middle are shown the two variants with a threefold axis and a mirror. Only in the second case (right) do variants differ only by a translation.

2.5. Summary of results for a terrace

The variants of an epitaxial structure that appear by point symmetry on a single terrace each reflect a rotational or mirror symmetry of the terrace that is not present in the epilayer symmetry. To cancel from the enumeration of variants, terrace and epilayer mirrors must be parallel within the resolution of the detection equipment. The multiplicity of translational variants, when detectable and independent of other symmetry operations, multiplies the number from point symmetries to give the total of observable variants. A principal point here is that the variants occur on a single terrace with equal probabilities, from symmetry. Multilevel surfaces and vicinal miscut offer two means to interfere with the otherwise equal populations, and these are the topics of Sections 3 and 4. In connection with variant control when growing compounds, even on a single terrace, we note that specific variants can often be eliminated by admitting the epilayer chemicals in a selected order, so that surface sites are saturated with a single atomic species.

3. Variants on multi-level surfaces

Surfaces normally comprise terraces at different levels that terminate at step edges. Height differences of this type evolve thermally over sufficiently large areas, leaving the single terrace of Section 2 a special case. The proportions in which variants occur may then change because step edges and successive terraces generally nucleate variants differently, and the single terrace behavior is lost. Moreover, variant distributions

become inhomogeneous, linked to the particular terrace type underlying the region. Unfortunately only a limited opportunity for manipulating variant populations arises from this selectivity. The behaviors differ for crystals with a single atom occupying each lattice point, which for convenience we call Bravais crystals, and crystals with a basis of two or more atoms. The cases are treated successively in what follows.

3.1. Multi-level Bravais substrate

To help define terms, Fig. 5 gives simplified sketches of multilevel Bravais substrates, some with epilayers. Fig. 5a shows a rough multilevel surface, with unevenly spaced steps of random sign that create a distribution of terrace heights. The surface in Fig. 5b lacks roughness but has a gradient and is termed miscut or vicinal, the topic of Section 4. The effects of multilevel structure on variants are indicated in Fig. 5c,d. For chemical reasons nucleation generally occurs faster at steps than on terraces. Each step nucleates particular variants preferentially, whereas terraces nucleate all variants equally. Thus, in Fig. 5c,d, larger domains grow at step edges, downhill steps are shown nucleating variant 1 preferentially, while uphill steps correspondingly nucleate variant 2. For the miscut surface shown in Fig. 5c this results in a preponderance of variant 1 that is the focus of interest in Section 4. What follows concerns the behavior of variants on the multilevel surface with no average miscut, shown in Fig. 5d.

The terraces of a Bravais crystal substrate with surface normal $\mathbf{g}_s$(h,k,l) have identical atomic structures spanned by the in-plane basis vectors $\boldsymbol{a}_2^e$, $\boldsymbol{a}_3^e$, and connect to other terrace by means of the third basis vector $\boldsymbol{a}_1^s$. For the low-index planes this is a near-neighbor vector with a substantial component normal to the surface. For any given step edge, symmetry operations of the terrace must generate other step orientations equivalent to the first; the step distribution mirrors the terrace symmetry because step edges lie along atomic rows. For each category of step, equivalent steps occur with equal probability on a surface, which remains planar on average, and lacks azimuthal bias.

Although variants nucleate preferentially on steps (Fig. 5d), the conformity of the step orientations and variants to the terrace symmetry ensures that all point symmetries of terrace-nucleated variants must be nucleated at the steps, and with equal probabilities for a planar unbiassed surface. For each category of step we conclude finally that the steps that surround a terrace must, on average, contribute point symmetries of variants on the terrace with the same (equal) distribution as from terrace nucleation itself. In short, *the results of* Table 1 *for variant nucleation on the single terrace remain valid for the multi-level surface* for this special case of a Bravais crystal.

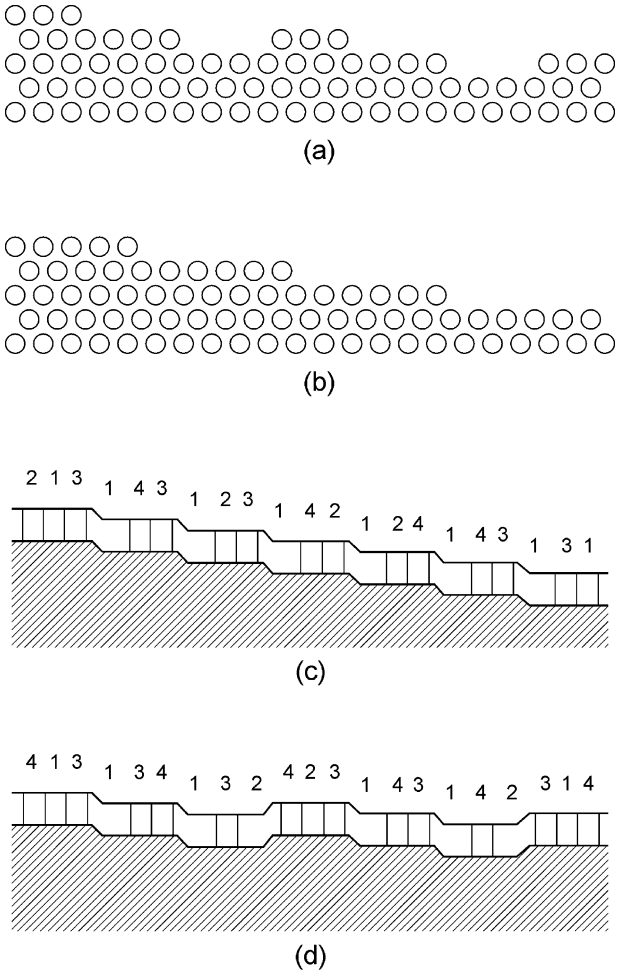

Fig. 5. The surface in (a) is rough while that in (b) remains miscut but lacks roughness, and so retains translational invariance. For the smoothly miscut surface in (c) the step edges nucleate the preferred variant, labeled 1, and this variant competes with nucleation of variants 1–4 on the terraces. In (d), the opposing steps caused by roughness nucleate variant 2, and the excess nucleation of the preferred variant, 1, from miscut competes with combined nucleation from terraces and from roughness.

Conversely, for Bravais crystals we conclude that multilevel effects on surfaces that lack azimuthal bias offer no opportunity to manipulate variant populations.

3.2. Multi-level substrates with a basis

On a crystal with a multi-atom basis, the surface species on successive terraces may be displaced and chemically distinct. The results of Section 2.4 correctly describe the variants that grow on any specific terrace. However, the differing chemistries and geometries of terraces may create variants as a succession of distinct single-terrace behaviors spread over the substrate surface. Relevant ideas are sketched in Fig. 6 for a sub-

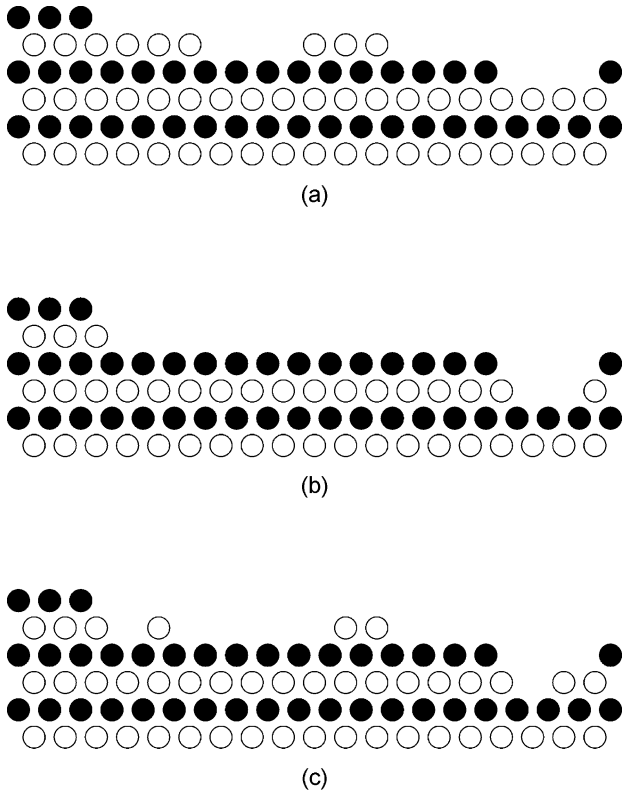

Fig. 6. Illustrative states of a multilevel surface with a basis. (a) shows a surface similar to Fig. 2a but with successive terraces made of an alternative species. The same surface is shown in (b) but with the entire basis removed at doubled step edges so that Bravais-like behavior results. In (c), one species is preferred but not uniquely present at the surface.

strate with two types of atom. Roughness and miscut can both reveal two distinct types of terrace, as illustrated in Fig. 6a. Bravais-like behavior can be recovered if, for chemical reasons, successive terraces differ by an entire basis unit, as shown in Fig. 6b. In most cases, however, thermal processes may break the basis in ways that vary from one terrace to the next. Therefore, the variant distribution (Fig. 6a) becomes a superposition of two chemically distinct forms. More generally (Fig. 6c) the surface structure and corresponding variant selection are still more heterogeneous.

As a real example, when GaAs grows on a Ge (001) terrace, after saturating with one component, say As, a single variant of GaAs occurs with As on levels $2n+1$ above the Ge terrace (at level 0) and Ga on levels $2n+2$, $n=0, 1, 2,...,$. On the next terrace up or down of the Ge substrate, the As still occurs first and so occupies levels $2n+2$, instead of Ga. Thus, the GaAs variant that forms there has the Ga and As atomic positions reversed from the variant on the first terrace. In this way successive terraces of substrates with a basis may nucleate distinct variants. Several, rather than just one, variant may occur on each terrace. When an epilayer lacking symmetry is grown on Ge (001) the 2mm terrace symmetry creates four variants interrelated by the two mirrors (Table 1). On the next terrace the structure is rotated through $\pi/2$ by the [001] screw axis, and the four variants take entirely new equivalent orientations, making eight variants in all. This happens also when the substrate contains more than one atomic species, for example replacing Ge with GaAs. The overall result even for Ge is that the variant population varies with location over the substrate surface, depending on the underlying terrace. This heterogeneity is, of course, greatest when the variants are smaller than a terrace width (Fig. 1).

We seek conditions under which particular variants may be suppressed. In two cases symmetry reveals when successive planes of a multilevel substrate with a basis have identical chemical activity, so that the desired specificity is clearly absent. First, successive planes can all be chemically identical only if *they each contain whole formula units* of the material. Second, in a material made from a single chemical species, but with more than one atom per unit cell, it is possible for the chemical equivalence of successive planes to be assured by the *symmetry of the atomic basis*. It is a fact that neither of these conditions is widely satisfied for compounds in general. Common structures like fluorite or perovskite with three or more atoms per formula unit do not possess even a single crystal plane that contains exact formula units [although, for example, (111) planes of Cu_3Au do]. Also, materials with a single atomic species in a structure with more than two sites per cell are rare. As a practical matter this has focused our attention on 'diatomic' crystals, with two atoms per cell. These contain many planes with whole formula units. They include much-studied lattices such as rocksalt, zincblende, and CsCl structures, with two dissimilar atoms as the basis, and diamond and h.c.p., which contain two identical atoms in positions related by symmetry operations. In what follows we treat crystals with two atoms per cell. The case of sapphire provides an example of more complex substrates which is outlined in Section 4.4 after the beneficial effects of substrate miscut are introduced.

3.3. Formula units of two chemically distinct atoms

Consider lattices with formula AB that contain just two inequivalent species A and B equally. Surface orientations of lattices with a basis are defined by planes of the underlying Bravais lattice. For crystals with formula AB, any given plane through an A atom passes through other A atoms located by $\boldsymbol{a}_2^s$, $\boldsymbol{a}_3^s$, and other spaced planes contain all remaining A atoms. The planes may: (1) contain B atoms also, in which case they contain all B atoms and the planes are all populated with the formula unit AB; or else (2) the first set of planes contains only A atoms and the A planes

are interleaved with B planes at spacings determined by the plane orientation and the basis vector. Roughness in the latter case exposes chemically heterogeneous surfaces, which can favor particular variants. To proceed we identify inactive surfaces occupied equally by A and B atoms.

Suppose that an A atom lies at the origin and that an associated B atom lies at

$$\boldsymbol{\rho} = x_1\mathbf{a}_1^s + x_2\mathbf{a}_2^s + x_3\mathbf{a}_3^s \tag{3}$$

with the $\boldsymbol{a}_i^s$ basis vectors of the lattice and the x_i (fractional) coordinates in the unit cell. Successive A planes of a specific orientation lie perpendicular to $\mathbf{g}(h,k,l)$, spaced by $d = 2\pi/|\mathbf{g}(h,k,l)|$ (see Section 2.1). Consequently, when the projection of $\boldsymbol{\rho}$ on $\mathbf{g}$ is nd, so that

$$\mathbf{g}\cdot\boldsymbol{\rho} = 2\pi n, \quad n, \text{integral} \tag{4}$$

the B atom must lie in a plane of A atoms n planes removed from the origin. Then all planes contain A and B atoms equally. Otherwise the A and B atoms lie in separate planes and neither type contains formula units. These results are now illustrated by application to f.c.c. and hexagonal materials.

3.3.1. Face centered cubic

This category includes zincblende and rocksalt crystals [32,33]. The scalar product in Eq. (4) can be evaluated using the fact that the body centered cubic reciprocal lattice occupies all points h, k, l, with h,k,l, either all odd or all even, of a simple cubic lattice of spacing $2\pi/a$ along cartesian coordinates with unit vectors **i**, **j**, **k**. With respect to these same coordinates the position vectors that locate the B atom relative to the A atom for rocksalt and zincblende, respectively, are:

$$\rho_R = a[\mathbf{i}+\mathbf{j}+\mathbf{k}]/2; \quad \rho_Z = a[\mathbf{i}+\mathbf{j}+\mathbf{k}]/4 \tag{5}$$

The scalar product of $\boldsymbol{\rho}$ with

$$\mathbf{g}_s(h,k,l) = 2\pi[h\mathbf{i}+k\mathbf{j}+l\mathbf{k}]/a \tag{6}$$

gives: for rocksalt: $h+k+l = 2n$;

$$\text{for zincblende: } h+k+l = 4n \tag{7}$$

in which the n are integers and h, k, l are all even or all odd. These values of $\mathbf{g}$ give the correct spacings of planes only for h, k, l from which all common factors are removed, so that possible solutions with all even coefficients must be designated in reduced form. The resulting planes that contain formula units are:

3.3.1.1. Rocksalt. All planes with either two of h, k, l odd and one even, or with one odd and two even; examples are (100), (110), (211) but not (111).

3.3.1.2. Zincblende. All planes with two of h, k, l odd and one even; examples are (110), (211), but not (100) or (111).

3.3.2. Cesium chloride

With its simple cubic Bravais lattice, CsCl has the same basis as NaCl, and h,k,l are confined to the same constraint as rocksalt, Eq. (7). Hence, if one of h, k, l, is even there is a single type of plane, and it contains whole formula units; examples are (110), (211). Otherwise there are two types of plane, e.g. for (100), (111).

3.3.3. Hexagonal

We analyze the case of hexagonal lattices for the special case of the WC structure [32,33], which has the same basis as hexagonal close packed (see Section 3.4) except that the two atoms of the basis are now different species. Thus,

$$\begin{aligned}&\rho = [4\mathbf{a}_1^s + 2\mathbf{a}_2^s + 3\mathbf{a}_3^s]/6;\\ &\mathbf{g}_s(h,k,l) = h\mathbf{b}_1^s + k\mathbf{b}_2^s + I\mathbf{b}_3^s\end{aligned} \tag{8}$$

and

$$\mathbf{g}\cdot\rho 3.4. = 2/3h + 1/3k + 1/2l = n \tag{9}$$

with n an integer. This is possible only if l is an even integer and $2h + k = 3n'$ with n' an integer. Examples are $(11\bar{2}0)$ and $(1\bar{1}\bar{2}2)$ but not $(1\bar{1}00)$.

For the conditions given above, the substrate (h, k, l) planes contain complete formula units and create identical rotational and mirror variants. The variants are displaced by interplanar translations $\boldsymbol{a}_1^s$, and whether this creates distinct translational variants or, alternatively, a single strained variant, is a matter to be decided case by case (Section 5.4). Results for various crystals are summarized in Section 4.5. Note that the criterion that planes contain whole formula units ensures identical planes only for diatomic crystals.

3.4. Diatomic crystals of a single chemical species

Substrate crystals with a basis AA′ of two chemically identical atoms separated by a position vector $\boldsymbol{\rho}$ also obey the results of Section 3.3, with two possible variants associated with the two sites. In addition, there are orientations in which the A and A′ atoms occupy separate, interleaved, planes and behave equivalently owing to a symmetry of the basis. Of interest are glide planes and screw axes [32] that pertain to the basis itself, in crystal structures termed non-symmorphic (as opposed to symmorphic crystals that lack these symmetry elements).

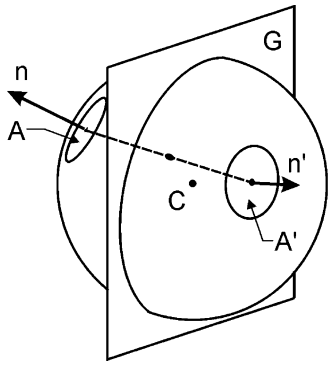

Fig. 7. The flat surfaces A and A′ are displaced images mirrored in the glide plane G, so that the two normals n and n′ are obtained from each other by reversing the component normal to G. When the two normals lie in the glide plane, A and A′ are successive planes of the same orientation.

3.4.1. Glide plane

The A′ sites are obtained when the A atoms undergo a given translation and are then reflected in a 'glide plane'. Surface planes are defined by the underlying Bravais lattice. Suppose initially that a given plane, normal **n**, is all A. Given the glide symmetry, there exists an equivalent plane, normal **n**′, containing all A′, which has the same surface normal with the component perpendicular to the glide plane G reversed (i.e. the plane is mirrored in the glide plane), as sketched in Fig. 7. From the mirror symmetry, any variant on the A plane must nucleate with the same probability as the displaced and mirrored variant does on the A′ plane. When the surface normals are confined to the glide plane the A and A′ planes are parallel and constitute successive terraces of a multi-terrace surface in the chosen orientation. Then variants related by the glide operation must nucleate equivalently on the successive terraces, and in identical proportions. When instead each plane contains A and A′ atoms equally, the same result holds between the two variants.

This glide-related equivalence persists, site by site, even when translational symmetry is broken, and the chemical activity of any site depends on its location (e.g. relative to a step edge). The mirror gives A and A′ planes equivalent, mirrored step edges, so that the plane and its partner under the glide operation retain equivalent nucleation characteristics, site by site, for the glide-related variants. In the case of two parallel planes, with normals in the glide plane, which are thus successive terraces for this orientation, the glide-related variants remain in equal proportions on successive terraces and step edges. This holds for all crystal planes with normals in glide planes. The same is true for A and A′ sites contained in a single plane. All planes with normals in a glide plane lack selectivity among variants, even when the activity varies with position on the terrace.

As one application we cite GaAs on Ge, whose diamond lattice has {001} glide planes with $\langle 110\rangle/4$ glide translations [32]. This glide operation transforms the two possible GaAs variants (with reversed Ga and As sites) one into the other. The preceding results show that when successive terraces are related by a glide operation, variants related by the same glide nucleate equivalently on the two terraces. In the present example, all {hk0} planes of arbitrary h and k have normals in (001) and, therefore, satisfy this requirement. Our discussion thus reproduces the analytical Pond result mentioned in the Introduction. Further planes not found in the Pond work are identified below. More important still is the use of the results for vicinal surfaces, discussed in Section 4.

In the h.c.p. lattice, $\{1\bar{1}00\}$ glide planes cut the triangular interstices of the close packed planes. Two variants of the WC lattice occupy the h.c.p. basis with dissimilar atoms in the two sites [31,32]. Our discussion shows that the two variants must nucleate equally on $\{hh\bar{2}h\,l\}$ planes, which all have normals in glide planes. Other planes break the symmetry so variants generally occur in unequal proportions.

3.4.2. Screw axis

The use of analogous methods for screw axes finds application only to those terraces that possess normals parallel to the screw axis (see Section 3.5).

3.4.3. Combined symmetries

The results may be deduced in alternative ways. From inversion and the $\langle 001\rangle$ Ge twofold axes, for example, one can show that two GaAs variants form equivalently for all surface normals that lie in the plane perpendicular to the rotation axes. These are of course the {hk0} planes, so the Pond result is again obtained. Results of multilevel behavior for a variety of crystal structures are collected in Section 3.6.

3.5. Multilevel effects on the global symmetry

Successive terraces of multilevel substrates with a basis generally differ in structure but not symmetry. Therefore, the global symmetry of variants on the entire surface often is the same as that for a single terrace. An exception occurs when the terrace is perpendicular to a screw axis of the substrate. Orientations of successive terraces then conform to the screw symmetry, and the variants on those terraces occur in orientations determined by the screw operation. The global symmetry of the surface is then the union of the global symmetry of the terrace and the rotational symmetry of the screw axis. Similarly, for epilayers, the axial translation that distinguishes an epilayer screw axis from a true rotation axis is lost in the global symmetry, and no distinction may be made between

epilayer screw and simple rotation axes. A case in point is Ge (001), which is perpendicular to a fourfold screw axis. Thus, the global symmetry of a multilevel Ge (001) substrate for variant enumeration is 4mm, while that of a single (001) terrace is 2mm.

3.6. Summary of results

Sections 3.3 and 3.4 provide orientations of multilevel diatomic crystals that, by symmetry, maintain equal populations of variants, just as do Bravais crystals (Section 3.1). Of greater interest are those remaining orientations, which discriminate among variants, and thereby offer the opportunity for experimental design. Table 2 collects results for various crystals with a basis of two atoms. Orientations that lack selectivity are listed under 'formula unit' or 'basis symmetry' when caused by formula units in the planes or by symmetry of the basis. The remaining low index planes, from which selectivity may be anticipated, are listed under 'active surfaces'.

The selectivity of the surfaces identified in Table 2 can arise from several alternative physical mechanisms. These include different surface areas occupied by the two types of terrace in equilibrium, since their differing chemistries generally bring different surface energies. Otherwise the differing nucleation and growth processes, both on the terraces and at their surrounding step edges, can create variant populations that differ between the two terrace types. On a rough but not miscut (Section 4) surface, all variants for a particular terrace occur equally, for reasons given in Section 3.1, so selectivity is lacking. Multilevel surfaces, therefore, offer most control when only one variant grows on each type of terrace. Materials tend to occur naturally with neutral surface planes (e.g. alkali halides), which make the smoothest templates. We mention that polar surfaces can nevertheless either occur with one species occupying almost all the terminating planes, e.g. for sapphire as Al_2O_3 (0001) [41], or can be prepared in that form [see, e.g. Barbier and Renaud [42] for NiO (111) and MgO (111)]. In effect the entire basis is removed at steps. As an example of a more complex substrate, the principal planes of sapphire are treated in Section 4.4.

4. Vicinal substrates

Step edges usually bind deposited species more strongly than do terrace sites. They bias variant populations as illustrated in Fig. 5. Of special interest here are experimental conditions under which a single variant can, by choice of miscut, be made to grow at the expense of other variants. For simple substrates, experimental studies of Cu_3Au (111) on Nb (110) demonstrate that a 1° miscut can eliminate almost all nuclei of a less favored (twin) variant even though the variants are equivalent on the terrace by symmetry [43]. Much earlier, experiments conducted on non-symmorphic crystals, apparently without reference to theory, but in conformity to the Pond result, found that single-domain GaAs (100) grew on Si (100) miscut along [011] [44], and along [211] [45], and later GaAs was grown on Ge (100) miscut along [011] [46]. For small miscuts two variants (antiphase domains) occur at low coverage on glide-related surfaces, but one grows out after 50 nm to leave a single variant; for tilts of 4° a single variant dominated throughout growth. Miscut has been equally effective when used for substrate and epilayer crystals with more complex structures. These include, for example, $Bi_2Sr_2Ca_{n-1}Cu_nO_{2n+4}$ grown on miscut $SrTiO_3$ [47] and on MgO (110) with CeO_2 buffer layers [48]. In some cases as above the epitaxial structure is unaffected by subsequent processing, but in others variants are formed by a structural phase transformation that makes the epilayer anisotropic *after* growth, during subsequent cooling, as in the case of $PbTiO_3$ grown on vicinal $SrTiO_3$ (001) [49]. The experimental research in the several areas has occurred independently and largely without reference to theory. Taken together, these experiments establish that miscut offers a power-

Table 2
Planes of diatomic crystals for which successive terraces are equivalent owing to the symmetry of the basis or because they contain formula units[a]

Substrate	Formula units	Basis symmetry	Active surfaces
Diamond	{110}{130}{211} {330}{332}	{100}{110}{120} {230}	{111}{113}{122} {133}
h.c.p.	{11$\bar{2}$0} {11$\bar{2}$2} {11$\bar{2}$2}	{0001} {11$\bar{2}$0} {11$\bar{2}$1} {11$\bar{2}$2}	{1$\bar{1}$00} {1$\bar{1}$01} {1$\bar{1}$02}
CsCl	{110}{211}		{100}{111}{210}
Rocksalt	{100}{110}{112} {123}{221}{223}		{111}{113}{133}
Zincblende	{110}{310}{211} {330}{332}		{100}{210}{111} {113}{221}{230}

[a] The final column lists remaining planes that yield generally inequivalent populations.

ful means to control variant populations. Details of growth on vicinal surfaces are revealed by low energy electron microscopy [50]. In what follows we consider Bravais crystals and multi-atom bases consecutively.

4.1. Miscut Bravais crystal substrate

The dependence of variant nucleation on vicinal miscut can be traced for sufficiently small miscut by noting that each step contributes its own bias to the net proportions of variants that are nucleated, in competition with both terrace nucleation and the nucleation at other step edges. The result is sketched for a vicinal crystal in Fig. 5c. For a crystal that lacks miscut the variants occur in equal proportions. Since extra steps of one type contribute additively for small miscut, the proportions of variants must vary linearly with the bias of steps, and hence linearly with miscut angle. Because the distribution of alternative steps depends on the miscut azimuth, the variant proportions also vary with miscut direction. Here we quantify the way symmetry constrains the variations.

Variant proportions depend on the orientation ϕ and size θ of the surface miscut vector $\mathbf{m} = \boldsymbol{\eta}\theta$. Here θ is the angle between the terrace normal and the normal to the average surface (i.e. the miscut angle) and ϕ is the angle unit vector $\boldsymbol{\eta}$ down the miscut gradient makes with a chosen reference. The fraction of variant α is written $f_\alpha(\theta,\phi)$, with α the substrate symmetry operation (not present in the epilayer) that creates variant α. If the behavior is linear for θ small, the steps create proportions $C\theta\, f_\alpha(\phi)$, with C constant. We now find the dependence of $f_\alpha(\phi)$ on ϕ as fixed by symmetry. There are two main points.

First, any symmetry elements that are *shared* by the substrate and the epilayer are symmetries of the entire system and belong to the $f_\alpha(\phi)$ also. For example, in a system with a fourfold substrate and a twofold epilayer, the miscuts $\mathbf{m}$ and $-\mathbf{m}$ are interchanged by a rotation π which leaves both the substrate and epilayer unchanged. The physical consequence is that the variant fraction $f_\alpha(\phi)$ also must have twofold symmetry in its dependence on ϕ. For similar reasons a mirror shared between the substrate and the epilayer introduce the same mirror into $f_\alpha(\phi)$.

The second point concerns symmetry elements of the substrate that are *not* shared by the epilayer. Being responsible for the variants, these operations may be identified by the label α of the variant to which each gives rise. *n* variants caused by an uncancelled *n*-fold rotational axis must exhibit equivalent behaviors. This means that only one independent fraction exists, say the first $f_0(\phi)$, while the remainder are obtained from

$$f_p(\phi - 2\pi p/n) = f_0(\phi), \quad p = 1,2...n-1 \tag{10}$$

Rotational symmetry alone creates no other constraint on variants.

A substrate mirror not present in the epilayer has further effect in $f_\alpha(\phi)$. Specifically, two variants created by the mirror must occur equally when the miscut vector coincides with the mirror plane. For other orientations of miscut the two variants occur in a ratio that is inverted for the mirror image miscut orientation. Specifically,

$$f_\alpha(\phi) = f_{\alpha'}(-\phi) \tag{11}$$

where ϕ is measured from the mirror plane.

When only two variants α and α' are created by a mirror, $f_\alpha + f_{\alpha'} = 1$ and the function

$$R_{\alpha\alpha'} = \ln[f_{\alpha'}(\phi)/f_\alpha(\phi)] \tag{12}$$

is an *odd* function of ϕ, as noted elsewhere [43]. This contrasts with the behavior of $f_\alpha(\phi)$ for a mirror which is present in *both* the epilayer and substrate, for which $R_{\alpha\alpha'}$ is *even* in $\phi - \phi_m$, in keeping with the discussion above. Experiments consistent with these results have appeared for Cu_3Au (111) epilayers, which are threefold with a mirror, grown with two (twin) variants on Nb (110) substrates which are twofold with a mirror, so that odd and even behaviors both occur. The observed bias on variant proportions becomes large only for miscuts exceeding $\sim 0.5°$, and for miscuts $\sim 1°$ one variant or the other is almost completely eliminated [43]. The behavior is qualitatively consistent with a terrace length of ~ 200 A from roughness and excess steps from miscut that eliminate almost all opposing steps as the miscut angle is increased. Similarly, miscuts $\sim 1°$ cause 'tuned tilt' [38] to saturate, with the opposing variant almost completely eliminated.

4.2. An example of variant proportions.

Little is known from experiment about the dependence of $f_\alpha(\phi)$ on ϕ. Nor does theory provide clear examples. Still, knowledge of $f_\alpha(\phi)$ in practical cases is a key ingredient in future efforts to eliminate unwanted variants from epitaxial materials. Here we describe a model that illustrates the strikingly anisotropic changes of variant population with miscut azimuth that occur within the symmetry restrictions described above.

We choose an epilayer that lacks symmetry grown on a substrate with a twofold axis and mirror (2 mm), so that four variants occur. To maximize anisotropic features we limit surface steps to the two directions $\boldsymbol{a}_2$ and $\boldsymbol{a}_3$ of nearest neighbors in the surface net (Fig. 6a inset), and postulate that each variant is created by only one type of step: variants ± 1 by $\pm\boldsymbol{a}_2$, respectively, and variants ± 2 by $\pm\boldsymbol{a}_3$, respectively. Here $\pm\boldsymbol{a}_2$ correspond to the two signs of step with edges parallel

to $\boldsymbol{a}_2$. Any miscut vector $\mathbf{m} = \boldsymbol{\eta}\theta$ corresponds to an average step orientation $\boldsymbol{l} = \boldsymbol{\eta}\ \mathbf{x}\ \mathbf{n}$ with $\mathbf{n}$ the terrace normal. This unit length of step is assumed to break into facets along $\boldsymbol{a}_2$ and $\boldsymbol{a}_3$ simply by projection, according to:

$$\mathbf{l} = \gamma_2 \boldsymbol{a}_2 + \gamma_3 \boldsymbol{a}_3 \tag{13}$$

in which

$$\gamma_2 = \mathbf{l}\mathbf{x}\boldsymbol{a}_3/\boldsymbol{a}_2\mathbf{x}\boldsymbol{a}_3; \qquad \gamma_3 = \mathbf{l}\mathbf{x}\boldsymbol{a}_2/\boldsymbol{a}_3\mathbf{x}\boldsymbol{a}_2 \tag{14}$$

The fractions of the variants are given by

$$f_\alpha(\phi) = \beta_\alpha/\Sigma_\alpha\beta_\alpha \tag{15}$$

We take two alternative models for the coefficients β_α which specify the relative rates at which the variants form. First (Model I) we examine the limit in which nucleation occurs only at step edges, with negligible terrace nucleation. For the mirror variants ± 1 nucleated on step edges $\pm \boldsymbol{a}_2$ we take: $\beta_{1+} = \gamma_2$ and $\beta_{1-} = 0$ when $\gamma_2 > 0$; and $\beta_{1-} = |\gamma_2|$ and $\beta_{1+} = 0$ when $\gamma_2 < 0$ (so that negative $\gamma_2 \boldsymbol{a}_2$ is taken as a *positive* coefficient multiplying the unit negative step, namely $-\boldsymbol{a}_2$). This is a reasonable model, with the nucleation rate of any variant proportional to the total length of the facet at which it nucleates. In a similar way the mirror variants ± 2 are nucleated on $\pm \boldsymbol{a}_3$. The results are shown as functions of ϕ in Fig. 8a, in which an uncancelled mirror plane is defined as $\phi_m = 0$.

As a second example, (Model II) illustrates the limiting regime of small miscut, again linear in θ, in which nucleation on the terraces (or at roughness) remains dominant. If the variants are nucleated equally, other than for the small perturbation due to nucleation on excess steps caused by miscut, the relative magnitudes of the latter terms are again given by Model I. Then

$$f_\alpha(\phi) = \beta'_\alpha/\Sigma_\alpha\beta'_\alpha \tag{16}$$

with modified coefficients

$$\beta'_\alpha = 1 + A\beta_\alpha \tag{17}$$

in which β_α has the value given above for model I and A is a constant (< 1) that fixes the (large) factor by which terrace- (or roughness)-nucleation exceeds step nucleation. The result of this calculation is given in Fig. 8b.

Fig. 8a,b both show how the mirror variants for each rotational label have complementary behavior, in agreement with the symmetry described above, and for both Model I and Model II. The fractions of the two rotational variants in each case differ by a rotation of π but are otherwise identical. The differences between

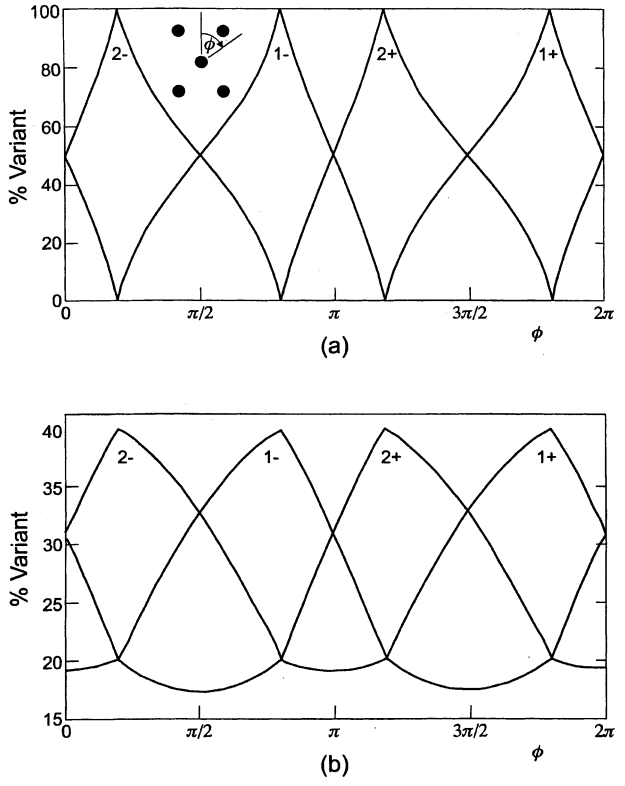

Fig. 8. The fractional occurrence of variants is shown as a function of angle ϕ for the four variants in the model described in the text. Part (a) gives the proportions when variants nucleate only on step edges and part (b) shows the case where nucleation on steps competes with the nucleation on terraces.

Fig. 8a and b illustrate the way physical mechanisms cause the angular variation to depend on the magnitude θ of the miscut, outside the linear regime. The reader is cautioned that the particular cases shown in Fig. 6 are illustrative results of microscopic models, but still reveal general features of symmetry-derived behavior.

Of particular interest is the way miscut offers the means to enhance the population of selected variants. It is notable that the model with (2mm) substrate symmetry and step nucleation only (Fig. 8a) does exhibit four orientations at which each variant, alone, is present. This ideal selectivity is surely not possible, however, with threefold or sixfold substrate symmetry because no miscut azimuth then selects one type of step uniquely. Nor can it occur if significant nucleation takes place on the terraces, as in Fig. 8b.

4.3. Miscut of crystals with a basis

The results for Bravais lattices remain valid for substrates of arbitrary complexity. Specifically, surface miscuts along any two orientations that are related by rotational or mirror symmetries of the substrate must result in equivalent proportions of two variants related

by the same substrate operations. The equivalence holds for any degree of substrate complexity. Section 4A remain valid regardless of how the miscut dissects the basis, because the equivalent dissection must occur at other symmetry-related azimuths. Of course a multilevel surface present at $\theta = 0$ may be chemically heterogeneous (see Fig. 6).

Further exact relationships for more complex crystals derive from the structure of the basis. Here we treat only systems with two atoms per cell for reasons analogous to those explained in Section 3, and consider chemically homogeneous systems first.

4.3.1. Vicinal crystals with a basis of two identical atoms

With only two similar atoms per cell, multilevel crystals (and hence vicinal crystals) nevertheless possess two distinct types of terrace unless all terraces contain exact formula units, as explained in Section 3.3. Otherwise, successive close packed step edges may have differing line energies that alternate, and the chemical processes that take place at the edges of the terraces differ for the two types of step edge. This is the case for variant nucleation on principal surfaces of even the simplest diatomic lattices. For Ge (001) miscut along $\langle 01\bar{1} \rangle$, for example, successive terraces have atoms at the $\langle 011 \rangle$ steps with bonds to atoms beneath that alternate, from one terrace to the next, between parallel and perpendicular to close packed steps (the surface chemistry gives rise to a 'dimer row' reconstruction [33] that alternates from one terrace to the next). Similarly, in the h.c.p. lattice, close packed steps on the (0001) surface have nearest neighbors from the plane below that alternate towards and away from the step on successive terraces. Very different physical [51] and chemical [52,53] characteristics may result for the two alternating types of step edge. The difference includes variant formation, so it is important to identify conditions that create the distinct chemical behaviors. As detailed in Section 3.3, the desired difference is maintained except when the two crystal planes that contain A and A′ sites have chemical behaviors that are mirror images in the glide plane, and are therefore equivalent by symmetry. The way vicinal miscut can be employed to break this symmetry is clearly a topic of interest.

The critical point is that glide-related variants are chemically equivalent only for step edges that are mirrors in the glide plane (so that the entire geometries of successive A and A′ planes are mirror images). But obviously this is possible only when the miscut is oriented in the glide plane. Therefore, even when successive planes are glide-related and thus equivalent, the equivalence can be broken by choice, by selecting a miscut directed along an azimuth that lies out of the glide plane, as with [011] for zincblende grown on (100) diamond planes. This valuable tool for the experimentalist who needs to tailor variant distributions has met with some success in practice [44–46].

The results summarized here complete the prescription for control of variant occurrence. A crystal with a glide plane creates two sets of variants whose members occur as pairs interrelated by the glide operation. Miscut discriminates among members of each set, as for Bravais lattices, even when the surface normal remains in a glide plane, and the degree of selectivity described in Section 4.2 remains accessible. When, in addition, the surface normal leaves the glide plane there is the further opportunity to control the proportions inside each glide-related pair, because the two glide-related variants are then no longer equivalent. Since symmetry-related alternative miscuts are available that interchange the behaviors of variant pairs, it is obvious in principle that the use of miscut offers the opportunity to enhance the population of any single, selected variant over all other variants. For this reason vicinal miscut is the most powerful tool for variant control available to the crystal grower.

4.3.2. Formula unit planes

When a multi-level crystal possesses a basis, it is shown in Section 3 that the variants remain equivalent for multilevel crystals on planes that contain complete formula units AA′ or AB. This multi-level constraint does not extend to all *miscut* crystals with formula unit planes. Specifically, successive steps may not be chemically identical, and this can create a heterogeneous distribution of variants.

The step edges are chemically identical for all miscut angles θ only for those directions of miscut that create step edges at which A and B atoms occur equally (in the truncated perfect crystal; the subsequent relaxation and thermalization does not affect the conclusions). To discuss this quantitatively we define basis vectors $\boldsymbol{b}_2^{\mathrm{s}}$, $\boldsymbol{b}_3^{\mathrm{s}}$, for the two-dimensional reciprocal lattice of the substrate surface net $\boldsymbol{a}_2^{\mathrm{s}}$, $\boldsymbol{a}_3^{\mathrm{s}}$. Here note that $\boldsymbol{b}_2^{\mathrm{s}}$, $\boldsymbol{b}_3^{\mathrm{s}}$, are coplanar with $\boldsymbol{a}_2^{\mathrm{s}}$, $\boldsymbol{a}_3^{\mathrm{s}}$, and differ from the three-dimensional reciprocal lattice vectors defined in Section 2. The vectors of the surface net reciprocal lattice are therefore

$$\boldsymbol{g}_{\mathrm{s}} = k\,\boldsymbol{b}_2^{\mathrm{s}} + l\,\boldsymbol{b}_3^{\mathrm{s}} \tag{18}$$

in which k and l are integers, and italic letters again identify properties of the surface net rather than the bulk Bravais lattice. The $\boldsymbol{g}_{\mathrm{s}}$ identify atomic rows by their in-plane normals

$$\boldsymbol{\eta} = \boldsymbol{g}_{\mathrm{s}}/|\boldsymbol{g}_{\mathrm{s}}| \tag{19}$$

Here, the *step* normal is identified with the *miscut* unit vector $\boldsymbol{\eta}$ that creates the particular step. An

in-plane position vector that connects A sites to B sites is

$$\boldsymbol{\rho} = x_2 \boldsymbol{a}_2^{\mathrm{s}} + x_3 \boldsymbol{a}_3^{\mathrm{s}} \tag{20}$$

with x_2, x_3, (fractional) coordinates in the surface unit cell. Then the condition that the successive step edges contain A and B equivalently is

$$\boldsymbol{g}^{\mathrm{s}} \cdot \boldsymbol{\rho} / 2\pi = x_2 k + x_3 l = n \tag{21}$$

with n an integer (as in Section 3.3). The fractions x_2, x_3, thus identify integers pairs h, k that make n an integer. From Eqs. (20) and (21) we then obtain the miscut unit vectors $\boldsymbol{\eta}$ for which successive step edges behave identically. Only for these directions of miscut does a formula-unit surface maintain its formula-unit character, with each step edge contributing variants in the same way. The results are particular to each individual surface orientation of every different crystal structure, and can be worked out as needed. The main point is that even crystals with formula unit terraces must generally nucleate variants unevenly when the terraces are miscut so that the two species do *not* appear in molecular combinations.

4.4. Sapphire: a complex but useful substrate

Here we analyze the characteristics of sapphire as a substrate material. This provides a useful example of more complex substrates. It gains relevance from the fact that four planes are commercially available in epitaxial grade material, and with vicinal miscuts selectable to 0.1°, and as a result have been employed in much epitaxial synthesis [54]. Their use in selecting epilayer symmetry is of evident interest. Note how the discussion necessarily passes from three-dimensional through two-dimensional symmetries for the several surface cuts in order to determine variant behavior.

Sapphire (Al_2O_3 or corundum) has the space group $R\bar{3}c$ (in full: $R\bar{3}c/2$; number 167 in the International Tables [55]). It is rhombohedral with two formula units per primitive cell. The conventional hexagonal cell contains three primitive cells. We consider the consequent symmetry constraints on (0001), $(1\bar{1}00)$, $(1\bar{1}02)$ and $(1\bar{1}20)$ planes as substrates, including activity induced by miscut.

4.4.1. (0001) substrates

The surface cut breaks the symmetry of the point group $\bar{3}$m, leaving 3m, and since the glide directions are not parallel to the surface, the terrace symmetry is just threefold (3). Going beyond symmetry alone, the surface is likely [38] to remain oxygen-terminated, and the six oxygens per cell occur in two planes that are glide-related and lie perpendicular to the c-axis. On a substrate lacking miscut, an epilayer with no symmetry will thus have six variants in two threefold sets related by a $\{1\bar{1}00\}$ glide plane; an epilayer mirror parallel to the substrate glide plane reduces the variants to three. Epilayers with 3 and 6 symmetry exhibit two mirror variants, one for each terrace, in proportions that vary with $[1\bar{1}00]$ miscut, while epilayers with 3m and 6mm symmetry occur with a single variant.

4.4.2. $(1\bar{1}00)$ substrates

This cut breaks all symmetry elements except one glide plane, with glide parallel to the c-axis. There is only one type of terrace, and epilayers that lack a mirror parallel to the glide plane exhibit two variants with proportions that vary with miscut perpendicular to the glide plane.

4.4.3. $(1\bar{1}02)$ substrates

Like $(1\bar{1}00)$, one glide plane has its glide parallel to the surface and creates two variants in epilayers that lack a mirror, in proportions that are tuned by miscut perpendicular to the glide plane. There are two Al planes and three O planes per repeat.

4.4.4. $(11\bar{2}0)$ substrates

All symmetry elements except a twofold axis are broken by this surface orientation. The Al ions lie in planes with single rows of sites empty, while the O ions lie in two slightly puckered planes. Each terrace has a twofold axis and accordingly creates two variants of epilayers that lack a twofold axis or a twofold screw axis normal to the surface; miscut tunes the proportions of these variants but its optimal azimuth is not fixed by symmetry alone. This is the surface on which useful buffers of (011) refractory bcc metals grow with [111] parallel to the missing Al rows [54].

4.5. Summary of results for vicinal miscut

Miscut can cause changes of variant populations. It can be employed to break a substrate symmetry, lacking in the epilayer, that would otherwise create unwanted variants. One of the most useful results available to the crystal grower seeking to eliminate variants created by substrate mirrors is that miscut along the mirror normal causes a repopulation of the two variants, related through the mirror, by complementary changes that are linear in the miscut angle θ, for θ small. Miscut that tilts the surface normal out of a glide plane discriminates between glide-related variants and can offer complete selectivity when only the two variants compete. Symmetry does not reveal which azimuth of miscut most enhances any chosen rotational variant, but directions perpendicular to atomic rows exhibit population maxima in the model calculations given above. Variant populations generally change linearly

with miscut angle except where they must, by symmetry, be even in θ.

5. Real crystals: symmetry results in the presence of defect structure

The purpose of this section is to show how the symmetry arguments used above hold up in real materials that contain symmetry-breaking defect structures.

5.1. Thermally activated structure

The surfaces of real substrates and epilayers support adatoms and advacancies in equilibrium proportions, and the surface species are displaced by relaxations[1] and reconstructions [56]. These complications are largely extraneous to the behavior of variants because of latent symmetries that reflect the symmetry of the ideal surface.

Our argument for all behavior activated by thermal fluctuations is exact and is presented in brief as follows. The Hamiltonians of the ideal crystals defined above possess precisely the two-dimensional symmetries identified in Section 2. Consequently, for each actual configuration and thermal process that breaks this symmetry, there exists an exactly analogous configuration and process in which the same symmetry breaking occurs, but operated on by any one of the identified symmetry operations to which the surface conforms. This applies clearly and precisely to all manner of site relaxations undergone by surface species, to all surface reconstructions and all configurations of surface point defects. Since the energetics and phase spaces of the equivalent configurations are exactly equivalent from symmetry, it follows that their average occurrences in thermal processes are identical. This being the case it is an *exact* conclusion that the average chemical products of all real surfaces that are thermal evolutions of any ideal surface, of a type considered above, retain precisely the same average symmetry as the ideal surface. This identity includes the occurrence of epitaxial variants, which is thus determined exactly by the symmetries of the ideal surface. Thus, Sections 2–4 remain valid in the presence of symmetry breaking in the thermal evolution of structure. The result is not confined to equilibrium but rather pertains to all thermal processes. Note that a close parallel exists between symmetry constraints for surface reconstructive transitions[1] [57] and for epilayers.

5.2. Variants at non-thermal defects

Consider variant generation at a particular non-equilibrium flaw in the otherwise ideal surface, and at a second equivalent flaw produced by operating on the first geometry with any one of the symmetry operations of the ideal surface. The two surfaces so created clearly have equivalent chemical behaviors, which includes variants related by the same symmetry operation.

Surface roughness often has athermal components caused by surface preparation. Provided that these features lack bias among equivalent crystal axes, they necessarily create the same uniform distribution of epilayer variants as the ideal terrace, as stated in Section 3. Second, for the biassed steps produced by miscut, the equivalent miscut produced by a substrate symmetry operation must create the equivalent surface chemistry, including variant generation, as stated in Section 4. These cases are to be distinguished from others which, while plausible, lack a fundamental basis. Specifically, it might be argued that arbitrary structural defects from random (and therefore unbiased) causes must give results (e.g. variants) that conform to the symmetry of the ideal surface. The argument amounts to a statement that the volumes of phase space for the equivalent events are equal, but in itself this certainly does not ensure the outcome in all instances.

5.3. Strain and incommensurability

Translational variants become hard to distinguish in normally strained and incommensurate [23–26] epilayers (the *bulk*, unstrained substrate and epilayer materials are invariably incommensurate). While the first monolayers may occupy sites of the substrate net pseudomorphically, beyond a critical thickness the epilayer transforms to a strained three-dimensional lattice and later relaxes by creation of 'misfit' dislocations that change the spacing at the interface. The results are quantified by a 'strain layer' model [58] which predicts as a function of thickness the epilayer relaxation required to minimize the strain and interfacial energy. In a sufficiently thin film the displacements parallel to the surface must be the same for all perpendicular positions; the equations of static elastic equilibrium [59] then have solutions that, when uniform in the plane of the interface, must be uniform in the third dimension also (specifically, through the film thickness). Then *an entire thin epilayer exists in a state of uniform but generally anisotropic elastic strain*. For variant domains only 10^3 atoms wide and misfits typically several percent,

[1] Much the same two-dimensional symmetry considerations apply to variants of epilayers and of reconstructions. Each also has inter-variant boundaries with specific line energies, and the variants induce stresses in the substrate in both cases. For both phenomena the result can be competing long and short range interactions that induce superstructure and can form stripe phases [57] in the surface configuration of lowest free energy; this influence epilayers only to the extent that the surface mobility is sufficient for the structures to respond to the interactions, which limits the relevance mainly to monolayers.

the resulting displacements are tens of atomic spacings. As a result epilayers are incommensurate with the substrate (except for thin layers in which the strain is unrelaxed), and no exact fit remains between atomic locations in the epilayer bulk and the substrate surface. Being very thick compared to the epilayer, the substrate remains in a state of uniform, but essentially zero, strain.

Incommensurability has no effect on variants derived from point symmetry operations, and the results of Sections 2–4 remain valid. Two points may be made about translational variants. First, the identification of translational variants with specific lattice sites may be lost. Second, interfacial structure may afford a means to identify the local translational state of the epilayer relative to the substrate lattice.

Suppose that the variant size is $D = Na$, with in-plane atom spacing a, and that the fractional misfit between the substrate and epilayer spacings is a strain ε. When $N\varepsilon > 1$, a strain larger than a lattice spacing occurs across a variant, so variants can no longer be associated with specific lattice sites. Visible domain boundaries may still distinguish alternative translational domains, all variants having the same shift, but the domains cannot be identified with specific substrate sites. When variants have coupled translational and point operations it seems best to identify them by the point operation so that the limitation on translational identification be avoided where possible.

The interfacial structure that decouples the epilayer spacing from the substrate may be detailed and complex, and attract much interest [18,60,61]. Many relevant features occur in the Frenkel-Kontorowa model; excellent reviews of this elaborate behavior are available [62]. The epilayer and substrate nets often remain partially coherent at their interface, with regions of almost perfect fit separated by defective material [60,61]. Growth instabilities in which strain causes non-planar growth fronts [63,64] are neglected here. The translational states of variants are most easily observed for thin pseudomorphic films where the registry and misfit at boundaries among monolayer variants may be explored at atomic resolution, for example by scanning tunneling microscopy [65,66]. The point of interest here is that for a thick incommensurate film of low index, the interfacial registry and the interfacial line defects between commensurate regions of interface may both remain discernable. Examples are the interfacial networks for Ni_2Si on Si (111) observed by transmission electron microscopy [67], and for Ag on MgO (001) observed by grazing incidence X-ray diffraction [68]. These features can (in principle) be employed to classify translationally dissimilar interfacial regions even for an incommensurate epilayer.

In summary, translational variants in thick epilayers usually cannot be classified by substrate sites. It may still be possible to identify translational states by *interfacial* structure, using line defects among coherent interfacial regions smaller than the variants.

5.4. Strain at step edges

When nucleation is limited, variants created on one terrace pass over step edges to cover neighboring terraces also, as in Fig. 1a. This has no effect on rotational and mirror variants, but can affect translational identities. The substrate and epilayer translation vectors $\boldsymbol{a}_1^e$, $\boldsymbol{a}_1^s$, between terraces generally differ, and step edges act as nuclei of strain in both the substrate and epilayer even for Bravais lattices (still larger differences may occur when the vectors $\boldsymbol{\rho}$ of multi-atom bases are involved). The character of these interfacial defects is discussed by Hirth and Pond [20] and Sutton and Balluffi [18]. In size the perpendicular component of misfit is a fraction of the step height. For MgO (001) grown rotated 45° on b.c.c. V (001) the substrate and epilayer planes differ in thickness [69] by a factor as large as $\sqrt{2}$. Such shifts are comparable with the displacements between variants, so substrate steps interfere with the identification of translational variants. The difficulties increase for high indices. When $\mathbf{g}$(h,k,l) is large and the plane spacing $d = 2\pi/|\mathbf{g}|$ is correspondingly small, the vectors $\boldsymbol{a}_2^s$, $\boldsymbol{a}_3^s$ of the surface net are large multiples of $\mathbf{a}_1^s$, $\mathbf{a}_2^s$, $\mathbf{a}_3^s$, so that the substrate and epilayer displacements at a step edge may differ by interatomic distances.

In summary, the displacements caused by steps contribute to epitaxial strain and tilt, but do not seriously influence rotational and mirror variants (the results of Sections 2–4 for variants from point symmetry remain valid). Epilayer registry is nevertheless degraded and translational identities may be lost.

6. Applications

The main purpose of this paper is to provide a comprehensive and accessible treatment of variants that form during heteroepitaxy. It is our expectation that, with the results presented here, most examples of variant formation met in practical cases can be understood and analyzed by inspection alone.

Variants often appear as undesirable structures that break translational symmetry and scatter elementary excitations unnecessarily. In this paper we detail the steps available to control variant formation. Particular orientations of miscut that differentiate effectively among the populations of variants are identified from symmetry; those that are ineffective may be avoided. The experimental application of these ideas remains at present in its infancy. We, nevertheless, visualize that different mechanisms by which multilevel structure affects variants will eventually be identified and the de-

tailed processes explored. For example, step-doubling caused by substrate energetics, and nucleation kinetics that originate in reactivity, must generally exhibit different chemical and temperature signatures that remain as yet to be identified in detail and employed in systematic epitaxial synthesis.

Acknowledgements

This research was supported in part by the Department of Energy through the University of Illinois Materials Research Laboratory, grant DEFG02-91ER45439.

Appendix A. Symmetries of the epilayer

While the substrate is semi-infinite with a single surface, a thin film epilayer may reasonably be modeled as a slab with both upper and lower surfaces. The new symmetry elements thus, introduced are of interest and are discussed briefly here.

The symmetry elements not present for a two-dimensional crystal are: a twofold rotation axis parallel to the slab (m′ or 2); a mirror with normal along the surface normal (1′ or m); an inversion center (2′ or $\bar{1}$); the inversion axes $\bar{3}$, $\bar{4}$, 6′ or $\bar{3}$ and 4′ or $\bar{4}$ (the twofold axis $\bar{2}$ is equivalent to a mirror and the sixfold axis $\bar{6}$ to a threefold axis with a perpendicular mirror, so they can be ignored). Where two symbols are given the first is a symmetry operation for a layer and the second for the point group. All inversion axes of a slab have the axis perpendicular to the surface. The symmetry operations of the epilayer form a group. The groups are isomorphic onto the group of periodic patterns with patterns on both sides of the paper (the point groups of diperiodic plane figures), onto the diffraction groups [66], and onto the two dimensional two-color point groups. These are the 31 groups listed in Table 3.

A comment is required about screw axes perpendicular to the surface, and glide in any plane that contains the surface normal. Suppose that the substrate has a threefold rotation axis and the epilayer has a threefold screw axis. Then the epilayer goes down in three orientations which are identical except for displacements normal to the surface. To the degree that strain at their interfaces can be accommodated (Section 5.4), this distinction can be ignored, and a substrate or epilayer screw axis may be treated as a rotation axis of the same order, just as glide planes can be treated as simple mirrors.

The variants created by a mirror are enantiomorphs of the originals, related by the change from right handed to left handed axes. They have the same chemical configuration and surface properties, and bear the same relationship to the substrate, whose structure conforms to the mirror. Thus, they may reasonably be termed variants. In some cases they have the same structure as the originals. This happens when the epilayer also contains a mirror perpendicular to the surface. The reflection between the variants is then equivalent to

Table 3
Symmetries of the epilayer[a]

White			Grey (m added)			B and W (2 added)			B and W (Inv added)		
1	1	E*	1′	m	I	m′	2	E*	2′	$\bar{1}$	I
m	m		m1′	2 mm		2′mm′	2/m				
2	2	E	21′	2/m	I	2 m′m′	222	E*	4′	$\bar{4}$	I
2 mm	2 mm		2 mm1′	mmm		4′mm′	$\bar{4}$2 m				
3	3	E	31′	$\bar{6}$	I	3 m′	32	E	6′	$\bar{3}$	I
3 m	3 m		3m1′	$\bar{6}$m2		6′mm′	$\bar{3}$ m				
4	4	E	41′	4/m	I	4 m′m′	422	E			
4 mm	4 mm		4mm1′	4/mmm							
6	6	E	61′	6/m	I	6 m′m′	622	E			
6 mm	6 mm		6 mm1′	6/mmm							

[a]The columns are in sets of three in which the left entry is the standard symbol for a point group of the diperiodic plane figures, the middle column is the symbol for the same symmetry in the standard form for crystallographic point groups, and the third column gives information about the group. The first set of columns gives the 10 'white' groups, which are the point groups of one-sided figures (the same as for the substrate). The members of the second set of columns are the 'grey' groups, which have a mirror parallel to the layering added to the white groups. For the 11 remaining 'black and white' groups the surfaces are interchanged without a mirror. The third set of columns are symmetries derived from the white groups by an added twofold axis parallel to the layers. The last column gives the three groups that are formed by added inversion axes. Each horizontal row contains groups with the same plane symmetry and the same number of variants. Shaded rows contain groups with a vertical mirror so the variants are related by a rotation about the surface normal. Groups labeled I have an inversion axis and the variants are related by a rotation about a horizontal axis. Groups labeled E have neither a mirror nor a rotation axis. Those lacking an asterisk can arise only from enantiomorphous crystal point groups, so no rotation can bring one variant into coincidence with another. Those marked by an asterisk may or may not arise from an enantiomorphous point group. In the latter event there is a rotation that carries one variant into the other, but as it is neither parallel nor perpendicular to the layer it requires an epilayer cut from the crystal at a different orientation. The several possible epilayer symmetries for a given crystal point group have been tabulated by Buxton et al. [70] Tables 3 and 4.

rotation of the variant about the surface normal through twice the angle between the mirror in the substrate and the mirror in the epilayer. When the mirrors are parallel the two variants are degenerate and the substrate mirror creates no new variant. This accounts for 13 of the 31 groups in Table 3.

For the eight groups that have an inverting symmetry axis but no mirror perpendicular to the surface, the reflection between variants is equivalent to a rotation by π about an axis parallel to the slab, which turns the slab over. These eight groups are marked with an I in Table 3.

For the remaining 10 groups, no rotation can bring the variants into coincidence. For seven of the 10 groups the enantiomorphous variants come from enantiomorphous crystals. However, for the remaining three, namely 1, 2m′m′ or 222, and m′ or 2, the *variants* are enantiomorphs but the *crystals* may or may not be, depending on the point group of the crystal from which the epilayer is formed.

Suppose that the aim is to grow an optically active layer using one of the 10 enantiomorphous point groups identified above. It is necessary to choose a substrate that lacks the mirror, otherwise the result would be a mixture of variants with both senses of rotation.

References

[1] G. Van Tendeloo, S. Amelinckx, Acta Cryst. A30 (1974) 431.
[2] R.C. Pond, Proc. R. Soc. London A357 (1977) 471.
[3] R.C. Pond, W. Bollman, Phil. Trans. R. Soc. London A292 (1979) 449.
[4] V. Vitek, A.P. Sutton, D.A. Smith, R.C. Pond, in: R.W. Balluffi (Ed.), Grain Boundary Structure and Kinetics, ASM, Metals Park, Ohio, 1980.
[5] R.C. Pond, Inst. Phys. Conf. Ser. 57 (1983) 69.
[6] R.C. Pond, D.S. Vlachavas, Proc. R. Soc. London A386 (1983) 95.
[7] D. Cherns, R.C. Pond, Thin Films and Interfaces II, North-Holland, NY, 1984, p. 423.
[8] R.C. Pond, J.P. Gowers, D.B. Holt, B.A. Joyce, J.H. Neave, P.K. Larson, Thin Films and Interfaces II, North-Holland, NY, 1984, p. 273.
[9] R.C. Pond, J.P. Gowers, B.A. Joyce, Surf. Sci. 152/3 (1985) 1191.
[10] R.C. Pond, in: M. Loretto (Ed.), Dislocations and the Properties of Real Materials, Inst of Metals, London, 1985.
[11] R.C. Pond, in: F.R.N. Nabarro (Ed.), Dislocations in Solids, North Holland, Amsterdam, 1989.
[12] R.C. Pond, P.E. Dilbey, J. Phys. 51 (1990) C1–25.
[13] R.C. Pond, D.J. Bacon, A. Serra, A.P. Sutton, Metall. Trans. A22 (1991) 1185.
[14] J.W. Cahn, G. Kalonji, in: H.I. Aaronson (Ed.), Solid State Phase Transformations, ASM Metals Park, Ohio, 1982.
[15] G. Kalonji, J.W. Cahn, J. Phys. 43 (1982) C6–25.
[16] S.-W. Chan, J. Phys. Chem. Solids 55 (1994) 1137.
[17] M. Guymont, D. Gratias, R. Portier, M. Fayard, Phys. Stat. Sol. A38 (1976) 629.
[18] A.P. Sutton, R.W. Balluffi, Interfaces in Crystalline Solids, Oxford UP, Oxford, 1995.
[19] W. Bollmann, Crystal Defects and Crystalline Interfaces, Springer, Berlin, 1970.
[20] R.C. Pond, J.P. Hirth, in: H. Ehrenreich, D. Turnbull (Eds.), Solid State Physics v 47, Academic Press, NY, 1994.
[21] K.V. O'Donovan, R.S. Beach, M.B. Salamon, C.P. Flynn, J. Magn. Mag. Mater. 186 (1998) 161.
[22] R.W. Erwin, J.J. Rhyne, M.B. Salamon, J. Borchers, S. Sinha, R.-R. Du, C.P. Flynn, Phys.Rev. B35 (1987) 6808.
[23] J.W. Matthews, Epitaxial Growth, Academic, NY, 1975.
[24] J.M. Gibson, L.R. Dawson (Eds.), Layered Structures, Epitaxy and Interfaces, Materials Research Society, Pittsburgh, 1985.
[25] M.A. Herman, H. Sitter, Molecular Beam Epitaxy, Springer, Berlin, 1996.
[26] A. Pimpinelli, J. Villain, Physics of Crystal Growth, Cambridge UP, Cambridge, 1998.
[27] J.C.A. Huang, R.-R. Du, C.P. Flynn, Phys. Rev. Lett. 66 (1991) 341.
[28] R.F.C. Farrow, J. Vac. Sci. Technol. B1 (1983) 222.
[29] J.M. Poate, K.N. Tu, J.W. Mayer (Eds.), Thin Films — Interdiffusion and Reactions, Wiley, NY, 1978.
[30] J.M. Ziman, Principles of the Theory of SolidsCambridge, 1964.
[31] F.S. Galasso, Structure and Properties of Inorganic Solids, Pergamon, Oxford UP, Oxford, 1970.
[32] C. Hammond, The Basics of Crystallography and Diffraction, Oxford UP, Oxford, 1997.
[33] J.E. Griffith, G.P. Kochanski, Crit. Rev. Solid State Mater. Sci. 16 (1990) 255.
[34] R. Schuster, J.V. Barth, G. Ertl, R.J. Behm, Phys. Rev. B44 (1991) 13689.
[35] R. Koch, E. Schwartz, K. Schmidt, B. Burg, K. Christmann, K.H. Rieder, Phys. Rev. Lett. 71 (1993) 1047.
[36] G.C. Shaw, S.C. Fain, M.D. Chin, Phys. Rev. Lett. 41 (1978) 955.
[37] J.P. McTague, A.D. Novaco, Phys. Rev. B19 (1979) 5299.
[38] C.P. Flynn, MRS Bull. 16 (1991) 30.
[39] K.E. Johnson, R.J. Wilson, S. Chang, Phys. Rev. Lett. 71 (1993) 1055.
[40] R.A. McKee, F.J. Walker, E.D. Specht, G.E. Jellison, L.A. Boatner, Phys. Rev. Lett. 72 (1994) 2741.
[41] P. Guenard, G. Renaud, A. Barbier, M. Gautier-Soyer, Surf. Rev. Lett. 5 (1997) 321.
[42] A. Barbier, G. Renaud, Surf. Sci. 392 (1997) L15.
[43] S.W. Bonham, C.P. Flynn, Phys. Rev. B58 (1998) 10875.
[44] R. Fischer, N. Chand, W. Kopp, H. Morkoc, L.P. Erickson, R. Youngman, Appl. Phys. Lett. 47 (1985) 397.
[45] P.N. Uppal, H. Kroemer, J. Appl. Phys. 58 (1995) 2195.
[46] S. Strite, M.S. Unlu, G.-B. Gao, A. Agerwal, A. Rockett, H. Morkoc, D. Li, Y. Nakamura, N. Otsuka, J. Vac. Sci. Technol. B8 (1990) 1131.
[47] J.N. Eckstein, I. Bozovic, D.G. Schlom, J.S. Harris, Appl. Phys. Lett. 57 (1990) 1049.
[48] J. Tanimura, K. Kuroda, M. Kataoka, O. Wada, T. Takami, K. Kojima, T. Ogama, Jpn. J. Appl. Phys. 32 (2) (1993) L254.
[49] C.D. Theis, D.G. Schlom, J. Mater. Res. 12 (1997) 1297.
[50] E. Bauer, Rep. Prog. Phys. 57 (1994) 895.
[51] M.G. Lagally, Y.W. Mo, R. Koriotis, B.S. Swartzentruber, M.B. Webb, in: M.G. Lagally (Ed.), Kinetics of Order and Growth at Surfaces, Plenum, NY, 1990.
[52] D.E. Jones, J.P. Pelz, Y. Hong, E. Bauer, I.S.T. Tsong, Phys. Rev. Lett. 77 (1996) 330.
[53] J.B. Hannon, B.S. Swartzentruber, G.L. Kellogg, N.C. Bartlett, Surf. Rev. Lett. 5 (1998) 1159.
[54] Some applications are summarized by C.P. Flynn, M.B. Salamon, in: K.A. Gschneidner, L. Eyring (Eds.), Handbook of

Physics and Chemistry of Rare Earths, vol. 22 Elsevier, Amsterdam, 1996.
[55] L. Mui, in: T. Haken (Ed.), International Tables for Cystallography, Reidel, Dordrecht, 1983.
[56] P. Toledano, V. Dmitriev, Reconstructive Phase Transitions, World Scientific, Singapore, 1996.
[57] M. Seul, D. Andelman, Science 267 (1995) 476.
[58] B.W. Dodson, J.Y. Tsao, Ann. Rev. Mater. Sci. 19 (1989) 419.
[59] A.E.H. Love, The Mathematical Theory of Elasticity, Dover, NY, 1944.
[60] J.M. Howe, Interfaces in Materials, Wiley, NY, 1997.
[61] H. Luth, Surfaces and Interfaces of Solid Materials, Springer, Berlin, 1993.
[62] W. Selke, in: C. Domb, J.V. Lebowitz (Eds.), Phase Transitions and Critical Phenomena, vol. 15, Academic, NY, 1992.
[63] A.G. Cullis, D.J. Robbins, A.J. Pidduck, W.P. Smith, in: A.G. Cullis, N.J. Long (Eds.), Microscopy of Semiconducting Materials, vol. II, IP Conf Ser, 117, Bristol, 1991, p. 439.
[64] D.E. Jesson, S.J. Pennycook, J.-M. Baribeau, D.C. Houghton, Phys. Rev. Lett. 71 (1993) 1744.
[65] R. Wiesendanger, H.-J. Guntherodt, Scanning Tunneling Microscopy, vol. I, II and III, Springer, Berlin, 1993.
[66] F. Bessenbacher, Rep. Prog. Phys. 59 (1996) 1737.
[67] R.A. Hamm, J.M. Vandenberg, J.M. Gibson, R.T. Tung, in: R.W. Balluffi (Ed.), Grain Boundary Structure and Kinetics, ASM, Metals Park, Ohio, 1980.
[68] G. Renaud, P. Guenard, A. Barbier, Phys. Rev. B58 (1998) 7310.
[69] C.P. Flynn, S. Yadavalli, Acta Metall. Mater. 40 (1992) S45.
[70] B.F. Buxton, J.A. Eades, J.W. Steeds, G.M. Rackham, Phil. Trans. A281 (1974) 171.